NACA

RESEARCH MEMORANDUM

AERODYNAMIC CHARACTERISTICS OF A FULL-SPAN TRAILING-EDGE CONTROL ON A 60° DELTA WING WITH AND WITHOUT A SPOILER AT MACH NUMBER 1.61

By Douglas R. Lord and K. R. Czarnecki

Langley Aeronautical Laboratory
Langley Field, Va.

NATIONAL ADVISORY COMMITTEE
FOR AERONAUTICS

WASHINGTON
March 10, 1954

Classification cancelled (or changed to) Unclassified

By Authority of Nasa Tech Pub Announcement #123
(CHANGE)

7 Jan. 58

By [illegible] NK

GRADE OF OFFICER MAKING CHANGE

29 March 61
DATE

NATIONAL ADVISORY COMMITTEE FOR AERONAUTICS

RESEARCH MEMORANDUM

AERODYNAMIC CHARACTERISTICS OF A FULL-SPAN TRAILING-EDGE CONTROL ON A 60° DELTA WING WITH AND WITHOUT A SPOILER AT MACH NUMBER 1.61

By Douglas R. Lord and K. R. Czarnecki

SUMMARY

An investigation has been made at a Mach number of 1.61 and a Reynolds number of 4.2×10^6 to determine the aerodynamic characteristics of a full-span trailing-edge control on a 60° delta wing with and without a partial-span spoiler mounted on the wing just ahead of the control. Pressure distribution and hinge-moment measurements were made over an angle-of-attack range from 0° to 12° and a control deflection range from -30° to 30°.

The pressure-distribution results indicate regions of increased pressure due to flow separation ahead of the control at the larger control deflections and also ahead of the spoiler. Deflecting the control has no effect on the pressures measured ahead of the spoiler. In turn, the spoiler has no effect on the pressures measured over the control when the control is deflected away from the spoiler.

The control effectiveness and hinge-moment results indicate that the linear theory overestimates the effect of control deflection and angle of attack for the basic wing-control configuration. The spoiler investigated produced additional lift or roll control when used in conjunction with the full-span control without causing an increase in control hinge moment, or decreased the control hinge moment while maintaining the lift or roll control produced by the control alone.

INTRODUCTION

As part of a general program of research on controls an investigation is under way in the Langley 4- by 4-foot supersonic pressure tunnel to determine the important parameters in the design of controls for use on a delta wing at supersonic speeds. The first results of the tests,

reported in reference 1, showed the effect of control plan form and hinge-line location on the hinge-moment characteristics for a series of tip controls on a 60° delta wing at M = 1.61. More recent results, reported in reference 2, showed the effect of chordwise fences and attached tabs on the hinge-moment characteristics for one of the tip controls of reference 1 at a Mach number of 1.61.

Further tests have been made to determine the aerodynamic characteristics of a full-span trailing-edge control on the same 60° delta wing used in the previous tests. In view of the encouraging outlook on the use of spoilers as lateral control devices (for example, see ref. 3), the effect of a spoiler attached to the surface of the wing just ahead of the control hinge line was also studied. The results of these tests are presented in this paper.

The wing angle-of-attack range was from 0° to 12° and the control deflection range, relative to the wing, was from -30° to 30°. The tests were conducted at a Mach number of 1.61 and at a Reynolds number of 4.2×10^6, based on the wing mean aerodynamic chord of 12.10 inches. The control hinge moments were measured directly by means of strain gages, and the flow and control effectiveness characteristics were determined from pressure-distribution measurements.

SYMBOLS

M	stream Mach number
q	stream dynamic pressure
p	stream static pressure
p_l	local surface pressure
P	pressure coefficient, $\frac{p_l - p}{q}$
ΔP	increment in P across spoiler
α	wing angle of attack
δ	control deflection relative to wing (positive when control trailing edge is deflected down)
x	distance from wing apex in chordwise direction
y	distance from wing apex in spanwise direction

$\bar{c}$	wing mean aerodynamic chord
c_R	wing root chord
b/2	wing semispan
S	semispan-wing plan-form area
Q	moment of area of control surface about hinge line
L	semispan-wing lift
B	semispan-wing root bending moment
M'	semispan-wing pitching moment about 50 percent station of wing mean aerodynamic chord
H	control hinge moment about hinge line
C_L	lift coefficient, L/qS
C_b	root bending-moment coefficient, $B/2Sbq$
C_m	pitching-moment coefficient, $M'/qS\bar{c}$
C_h	hinge-moment coefficient, $H/2Qq$
ΔC_h	increment in C_h due to spoiler

APPARATUS

Wind Tunnel

This investigation was conducted in the Langley 4- by 4-foot supersonic pressure tunnel, which is a rectangular, closed-throat, single-return type of wind tunnel with provisions for the control of the pressure, temperature, and humidity of the enclosed air. For the tests reported herein, the nozzle walls were set for a Mach number of 1.6. At this Mach number, the test section has a width of 4.5 feet and a height of 4.4 feet. During the tests, the stagnation pressure was held at 15 lb/sq in, absolute and the dewpoint was kept below -20° F so that the effects of water condensation in the supersonic nozzle were negligible.

Model and Model Mounting

The model used in this investigation consisted of a half-delta wing having a full-span trailing-edge control surface 25 percent of the wing area. The control chord was the same as the partial-span trailing-edge control - configuration A - in reference 1. A spoiler of height equal to 5 percent of the wing mean aerodynamic chord and extending from the root chord outward to the 57.2 percent semispan station was mounted on the wing surface at the 82.5-percent station of the root chord for some of the tests. A sketch of the plan form and cross section of the basic wing with control showing the spoiler location is presented in figure 1.

The basic wing had a 60° sweptback leading edge, a root chord of 18.143 inches and a semispan of 10.475 inches. The wing had a rounded NACA 63-series section extending 30 percent root chord back from the leading edge, a constant-thickness center section with a thickness-chord ratio of 3 percent based on the root chord, and a sharp trailing edge. Near the wing tip, the nose section joined directly to the tapered trailing edge without any flat midsection.

The basic wing and control were constructed of steel with the pressure-tube installations made in grooves in the surface which were faired over with bismuth-tin alloy or with a plastic material. The 105 orifices were located at seven spanwise stations as shown in figure 1 and at chordwise positions listed in table I. All screw holes, pits, and mating lines were filled with dental plaster and faired smooth. The gap at the control hinge line was approximately 0.01 inch. The spoiler was made from 1/16-inch stock brass, bent to a right angle and attached to the wing surface so that the top of the spoiler was 0.605 inch from the wing surface.

The semispan wing with control was mounted horizontally in the tunnel from a turntable in a steel boundary-layer bypass plate which was located vertically in the test section about 10 inches from the side wall as shown in figures 2 and 3.

TECHNIQUES AND TESTS

The model angle of attack was changed by rotating the turntable in the bypass plate on which the wing was mounted. (See fig. 2.) The angle of attack was measured by a vernier on the outside of the tunnel, inasmuch as the angular deflection of the wing under load was negligible. Control deflection was changed by a gear mechanism mounted on the pressure box which rotated the strain-gage balance, the torque tube, and the control, as a unit. The control angles were set approximately with

the aid of an electrical control-position indicator mounted on the torque tube close to the wing root and were measured under load during testing with a cathetometer mounted outside the tunnel.

Control hinge moments were determined by means of an electrical strain-gage balance located in the pressure box (fig. 2) which measured the torque on the tube actuating the control surface. The pressure distributions were determined from photographs of the multiple-tube manometer boards to which the pressure leads from the model orifices were connected. The wing lift, pitching-moment, and bending-moment coefficients were determined from integrations of the pressure distributions. As a check on the control hinge-moment coefficients measured directly, values were also determined from the integrated pressure distributions.

Tests were actually made with the spoiler mounted on the upper surface only and at both positive and negative angles of attack. The data are presented as if the tests were made at 0°, 6°, and 12° angles of attack only, without the spoiler and with the spoiler mounted on either the upper or the lower surface of the wing. The control deflection range was from -30° to 30°, with hinge moments measured every 5° and pressure measurements every 10°. All tests were made at a tunnel stagnation pressure of 15 pounds per square inch corresponding to a Reynolds number, based on the mean aerodynamic chord of 12.10 inches, of 4.2×10^6.

PRECISION OF DATA

The mean Mach number in the region occupied by the model is estimated from calibration to be 1.61 with local variations being smaller than ±0.02. There is no evidence of any significant flow angularities. The overall accuracies of the integrated coefficients are not known; however, assuming the pressure-distribution fairings to be correct, the repeatability of the integrated coefficients and the estimated accuracies of other pertinent quantities are:

α, deg	±0.05
δ, deg	±0.1
P	±0.01
C_L (from integrations)	±0.005
C_D (from integrations)	±0.0025
C_m (from integrations)	±0.001
C_h (from direct measurements)	±0.005

[redacted]

RESULTS AND DISCUSSION

Pressure Distributions

Illustrative pressure distributions for the basic and spoiler configurations are presented in figure 4. Pressure distributions are shown for the three test angles of attack at zero control deflection and at the maximum positive and negative control deflections only. It should be pointed out that due to the limited number of orifices at each station, the fairings are somewhat arbitrary; however, trends can be seen.

Basic configuration.- Consider first the pressure distributions over the model without spoilers, as shown by the solid curves of figure 4. At a control deflection of 0°, an increase in angle of attack from 0° to 12° causes an increased loading over the entire chord at the inboard stations. This increase in loading is fairly uniform except near the leading edge, where localized upper-surface flow separation, characteristic of a subsonic leading edge, occurs. Outboard along the span, this upper-surface flow separation increases in chordwise extent until it covers the entire chord.

Deflection of the control to $\pm 30^\circ$ causes a large pressure rise on the wing ahead of the control high-pressure surface as a result of separation of the turbulent boundary layer. Although for purposes of simplicity, all the pressure distributions are not shown, this pressure rise does not appear until the control deflection approaches $\pm 20^\circ$, but then it moves rapidly forward with further increase in control deflection to $\pm 30^\circ$. When this separation is on the wing upper surface ($\delta = -30^\circ$), increasing angle of attack decreases the chordwise extent of the separated region. When the separation occurs on the wing lower surface ($\delta = 30^\circ$), increasing angle of attack causes the separation point to move farther forward. This result is more evident at stations 4 and 5 than at the inboard stations because of the lack of sufficient orifices in the separated region at the inboard stations.

Effect of spoiler.- With the control undeflected, figure 4 shows that the pressures ahead of the spoilers behave in a similar manner to the pressures ahead of the control when deflected 30°. The flow ahead of and behind a spoiler is described in detail in references 4 to 6.

In the present investigation, figure 4 shows that, at the inboard stations, the pressure rise ahead of the spoiler is very pronounced and extends for a considerable distance along the chord at all angles of attack, whether the spoiler is on the upper or lower wing surface. Outboard along the span, the magnitude and extent of the region of higher pressure seems to decrease ahead of the upper-surface spoiler.

With the spoiler installed, deflecting the control causes little change in the pressures measured ahead of the spoiler. When the control is deflected toward the spoiler, the pressure on the spoiler side of the control is much more negative than that measured on the basic configuration; however, the variation along the flap chord is similar to that attained on the basic configuration. When the control is deflected away from the spoiler, the pressures on the spoiler side of the control are very close to the pressures measured on the basic configuration.

The effect of angle of attack and control deflection on the expansion at the spoiler, which is an indication of the chord force on the spoiler, may be seen more clearly on the spanwise plots of incremental pressure coefficient across the spoiler shown in figure 5. For $\delta = 0^\circ$, increasing the angle of attack of the lower-surface spoiler configuration increases the pressure increment, the spanwise variation remaining fairly uniform. When the spoiler is on the upper surface, increasing the angle of attack decreases the pressure increment and at $\alpha = 12^\circ$, there is a large drop in pressure increment toward the outboard tip of the spoiler as a result of the wing leading-edge separation for this condition.

The lower part of figure 5 shows the effect of control deflection on the spoiler pressure increment for the upper-surface-spoiler configuration at $\alpha = 0^\circ$. For positive deflections, (that is, deflections away from the spoiler) there is little change in pressure increment. When the control is deflected toward the spoiler, (that is, negatively) the pressure increment decreases considerably.

Control Effectiveness

Basic configuration.- In figures 6 and 7 are shown the experimental and theoretical wing lift, bending-moment, and pitching-moment coefficient variations with control deflection and angle of attack for the basic configuration without spoilers. The theoretical curves were obtained by the linear-theory methods of references 7 and 8. From the plots of figures 6 and 7, it can be seen that the experimental variations with control deflection are all fairly linear except for some of the curves near the highest control deflections tested. In all cases, the linear theory overestimates the effect of control deflection by a considerable amount and overestimates the effect of angle of attack except for the pitching-moment coefficient (fig. 7(c)), for which linear theory predicts no change due to angle of attack. The lack of agreement between experimental and theoretical control effectiveness is the result of viscous effects and the limitations of the linear theory. The viscous loss in lift and bending moment is due primarily to the separation from the upper surface of the wing near the tip and separation from the low-pressure surface of the control over the

[redacted]

complete span. The change in pitching moment is due to the same factors and in addition is affected by the carryover of load ahead of the control hinge line, which results in a forward shift of the center of pressure for large control deflections.

Effect of spoiler.- The variations of wing lift, bending-moment, and pitching-moment coefficients with control deflection and angle of attack for the model having the spoiler on the upper surface are presented in figures 8 and 9. Similar plots for the lower-surface spoiler configuration are presented in figures 10 and 11. The variations for the basic configuration without spoiler are shown for comparison.

From figures 8 and 10 it is evident that when the control is deflected away from the spoiler, the slopes of the coefficient variations with δ are little affected by the spoiler. When the control is deflected toward the spoiler, the slopes of the coefficient variations with δ are decreased in magnitude.

From figures 9 and 11, it can be seen that the spoiler is most effective when projected in the opposite direction to the trailing-edge control deflection. For all control deflections, the spoilers have little effect on the slopes of the curves with angle of attack.

Spoiler control in conjunction with flap-type control.- From figures 8 to 11 it can be seen that over most of the angle range of the tests, projecting the spoiler on the proper surface could be used to increase the lift or rolling moment (bending moment) beyond that produced by the flap control alone. For this particular spoiler location, the spoiler helped the flap control develop pitch in only a small region near $\delta = 0^\circ$.

Spoiler control as compared with flap-type control.- Although only one spoiler configuration was tested during these tests, it may be of interest to compare the effectiveness of the spoiler in producing lift, bending-moment, and pitching-moment, with the effectiveness of the basic flap-type control. In figure 12 are shown the curves for the control deflection required on the basic configuration to produce the effectiveness given by the spoiler mounted on the upper or lower surface of the wing with the control undeflected. These curves show that, in general, the spoiler tested produces as much lift or bending moment as a flap-control deflection of from 4° to 8°, though analysis of the pressure distribution indicates that the spoiler would cause a much larger drag increment than would the deflected control. The spoiler tested is very ineffective for pitch control since the center of pressure of the incremental spoiler load is very near the moment center of the wing. It is to be expected that more rearward location of the spoiler would give more favorable pitch-control characteristics. It is entirely possible that improved overall effectiveness could be

obtained by other modifications, such as spoiler height, span, spanwise location, and sweep.

Control Hinge Moments

Basic configuration.- The experimental and theoretical hinge-moment-coefficient variations with control deflection and angle of attack for the basic configuration are presented in figure 13. In figure 13(a), the experimental data obtained from the integrated pressure distributions on the control are identified by the symbols, and the experimental data obtained from the strain-gage-balance measurements are identified by the solid curves. The agreement between the two methods of determining the hinge moments seems remarkably good, considering the small number of spanwise orifice stations. This should be indicative of the reliability of the effectiveness coefficients discussed previously, which were obtainable only from the pressure-distribution integrations.

The experimental variations of hinge-moment coefficient with δ are fairly linear except at the highest deflections tested, whereas the variations with α are all essentially linear. As was the case with the effectiveness predictions, the linear theory considerably overestimates the slopes of the hinge-moment coefficient curves with control deflection and angle of attack.

Effect of spoiler.- The variations of the control hinge-moment coefficient with control deflection and angle of attack are presented in figures 14 and 15 for the upper-surface and lower-surface spoiler configurations as compared with the variations for the basic configuration. The hinge-moment coefficients determined from the pressure distributions are again in fairly good agreement with those measured directly. The control hinge-moment coefficients measured with the spoilers installed on the wing are unchanged from those measured on the basic wing, except when the control is deflected toward the spoiler. For these conditions, appreciable reductions in the magnitude of the hinge-moment coefficients are obtained for the spoiler configurations.

The variations of these incremental hinge-moment coefficients with control deflection for the two spoiler configurations at the three test angles of attack are shown in more detail in figure 16. The change in the incremental variations with angle of attack was relatively small for the range investigated.

CONCLUDING REMARKS

An investigation has been made at a Mach number of 1.61 and a Reynolds number of 4.2×10^6 to determine the aerodynamic characteristics of a full-span trailing-edge control on a 60° delta wing with and without a partial-span spoiler mounted on the wing just ahead of the control. Tests were made at angles of attack from 0° to 12° and for control deflections from -30° to 30°.

The pressure distributions indicate large regions of increased pressure due to separation of the turbulent boundary layer ahead of the control at the larger control deflections and also ahead of the spoiler. Deflecting the control has no effect on the pressures measured ahead of the spoiler. In turn, the spoiler has no effect on the pressures measured over the control when the control is deflected away from the spoiler.

In general, the linear theory overestimates the effect of control deflection and angle of attack on the control effectiveness and hinge-moment coefficients of the basic wing-control configuration.

For most of the range of angles tested, the spoiler investigated produced additional lift or roll control when used in conjunction with the full-span control without causing any control hinge-moment penalty, or decreased the control hinge moment while maintaining the lift or roll control produced by the control alone.

Langley Aeronautical Laboratory,
National Advisory Committee for Aeronautics,
Langley Field, Va., December 1, 1953.

REFERENCES

1. Czarnecki, K. R. and Lord, Douglas R.: Hinge-Moment Characteristics for Several Tip Controls on a 60° Sweptback Delta Wing at Mach Number 1.61. NACA RM L52K28, 1953.

2. Czarnecki, K. R., and Lord, Douglas R.: Preliminary Investigation of the Effect of Fences and Balancing Tabs on the Hinge-Moment Characteristics of a Tip Control on a 60° Delta Wing at Mach Number 1.61. NACA RM L53D14, 1953.

3. Hammond, Alexander D.: Lateral-Control Investigation of Flap-Type and Spoiler-Type Controls on a Wing With Quarter-Chord-Line Sweepback of 60°, Aspect Ratio 2, Taper Ratio 0.6, and NACA 65A006 Airfoil Section - Transonic Bump Method. NACA RM L50E09, 1950.

4. Conner, D. William, and Mitchell, Meade H., Jr.: Effects of Spoiler on Airfoil Pressure Distribution and Effects of Size and Location of Spoilers on the Aerodynamic Characteristics of a Tapered Unswept Wing of Aspect Ratio 2.5 at a Mach Number of 1.90. NACA RM L50L20, 1951.

5. Patterson, R. L.: The Characteristics of Trailing-Edge Spoilers. Part II - The Effects of Gap, Flap Deflection Angle, Thickness, and Sweep Angle on the Aerodynamic Characteristics of Two-Dimensional Spoilers, and the Pressure Distribution Near the Tip of a Partial-Span Trailing-Edge Spoiler, at a Mach Number of 1.86 - TED No. TMB DE-3109. Aero. Report 827, David W. Taylor Model Basin, Navy Dept. Dec. 1952.

6. Mueller, James N.: Investigation of Spoilers at a Mach Number of 1.93 To Determine the Effects of Height and Chordwise Location on the Section Aerodynamic Characteristics of a Two-Dimensional Wing. NACA RM L52L31, 1953.

7. Tucker, Warren A., and Nelson, Robert L.: Theoretical Characteristics in Supersonic Flow of Two Types of Control Surfaces on Triangular Wings. NACA Rep. 939, 1949. (Supersedes NACA TN's 1600, 1601 and 1660.)

8. Ferri, Antonio: Elements of Aerodynamics of Supersonic Flows. The Macmillan Company, 1949.

TABLE I

CHORDWISE LOCATION OF ORIFICES

[Station spanwise locations shown in figure 1]

Orifice number	Station	x/c_R	Station	x/c_R	Station	x/c_R	Station	x/c_R	Station	x/c_R	Station	x/c_R	Station	x/c_R
1	1	0.048	2	0.210	3	0.372	4	0.537	5	0.592	6	0.745	7	0.867
2	1	.075	2	.238	3	.400	4	.562	5	.619	6	.772	7	.872
3	1	.219	2	.381	3	.538	4	.700	5	.713	6	.816	7	.910
4	1	.334	2	.502	3	.659	4	.860	5	.779	6	.860	7	.948
5	1	.445	2	.612	3	.747	4	.867	5	.860	6	.872	7	.986
6	1	.588	2	.756	3	.860	4	.872			6	.905		
7	1	.742	2	.860			4	.905			6	.949		
8	1	.860	2	.867			4	.949			6	.982		
9	1	.872	2	.872			4	.982						
10	1	.905	2	.905										
11	1	.949	2	.949										
12	1	.982	2	.982										

Orifice locations identical on upper and lower surface except as noted below.
Orifice number 1 is on leading edge at each station except at station 7.
Orifices located at $x/c_R = 0.867$ are on control leading edge.

Orifice Station	y (inches)	$\frac{2y}{b}$
1	.50	.048
2	2.20	.210
3	3.90	.372
4	5.62	.537
5	6.20	.592
6	7.80	.745
7	As shown	—

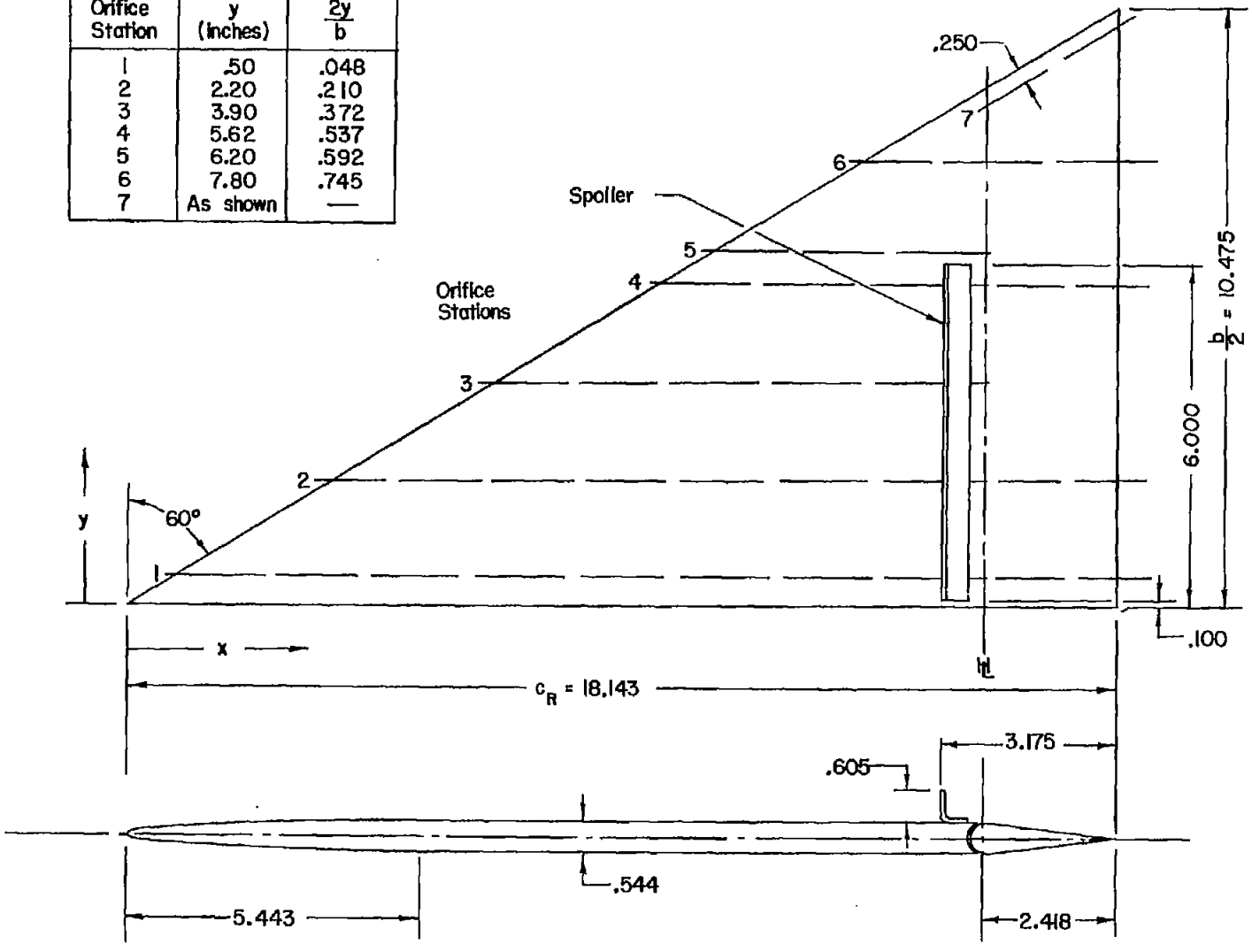

Figure 1.- Sketch of model configuration. (All dimensions in inches.)

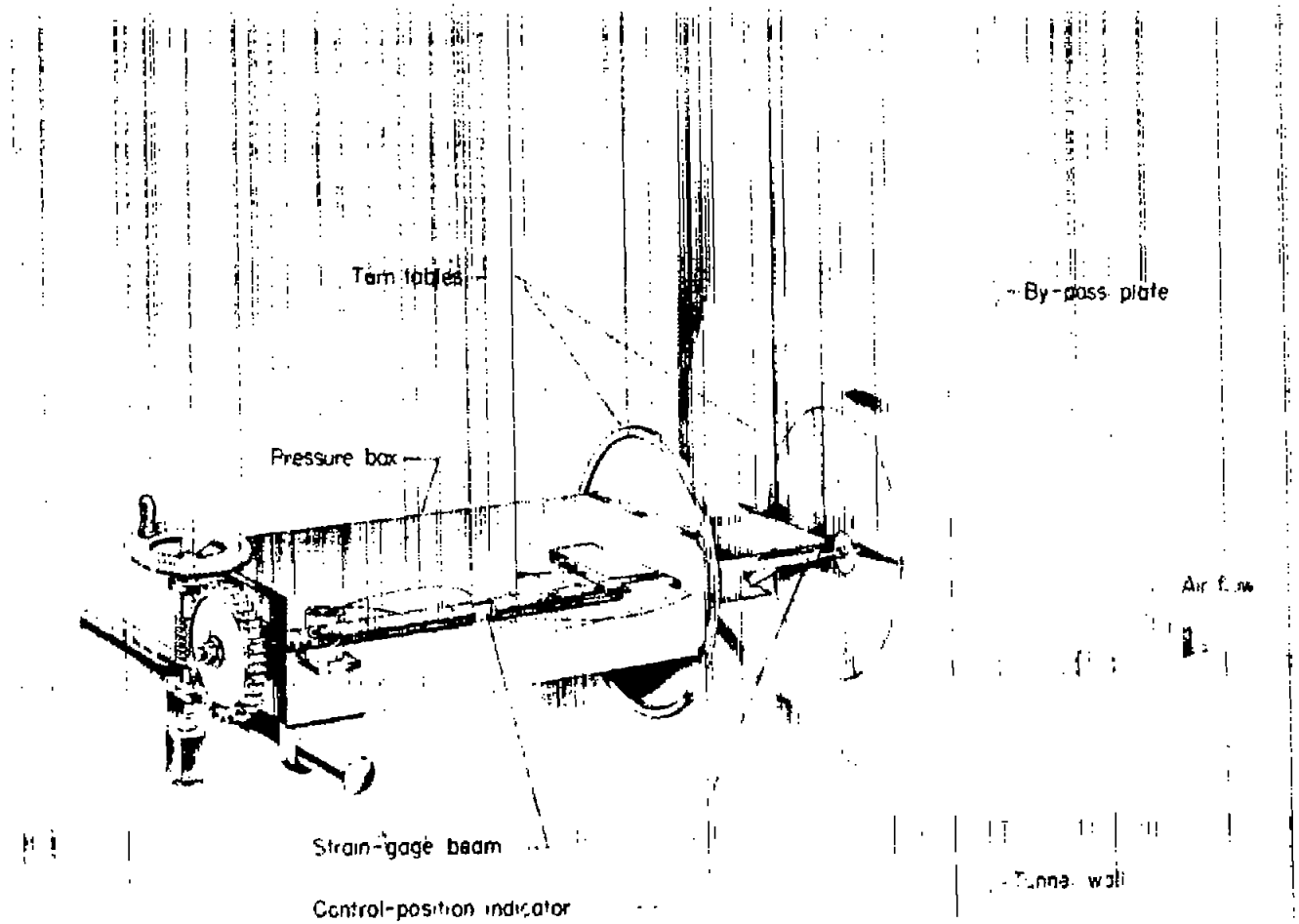

L-77038

Figure 2.- Sketch of test setup. Model shown not that of subject tests.

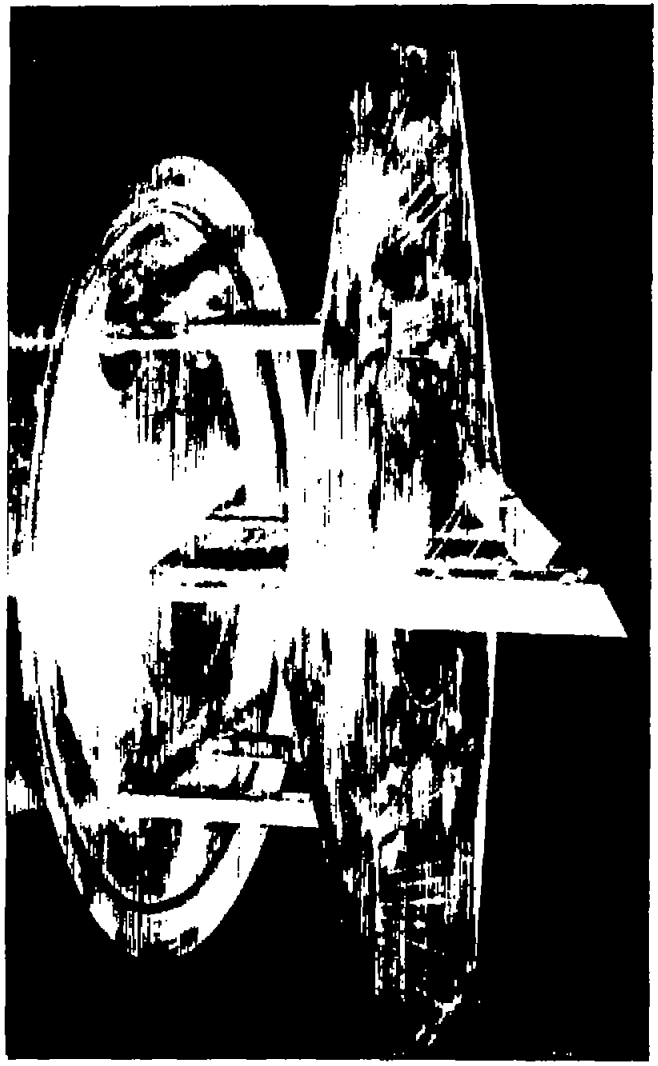

L-75295

L-75294

Figure 3.- Rear three-quarter and front three-quarter views of basic configuration mounted in tunnel on boundary-layer bypass plate.

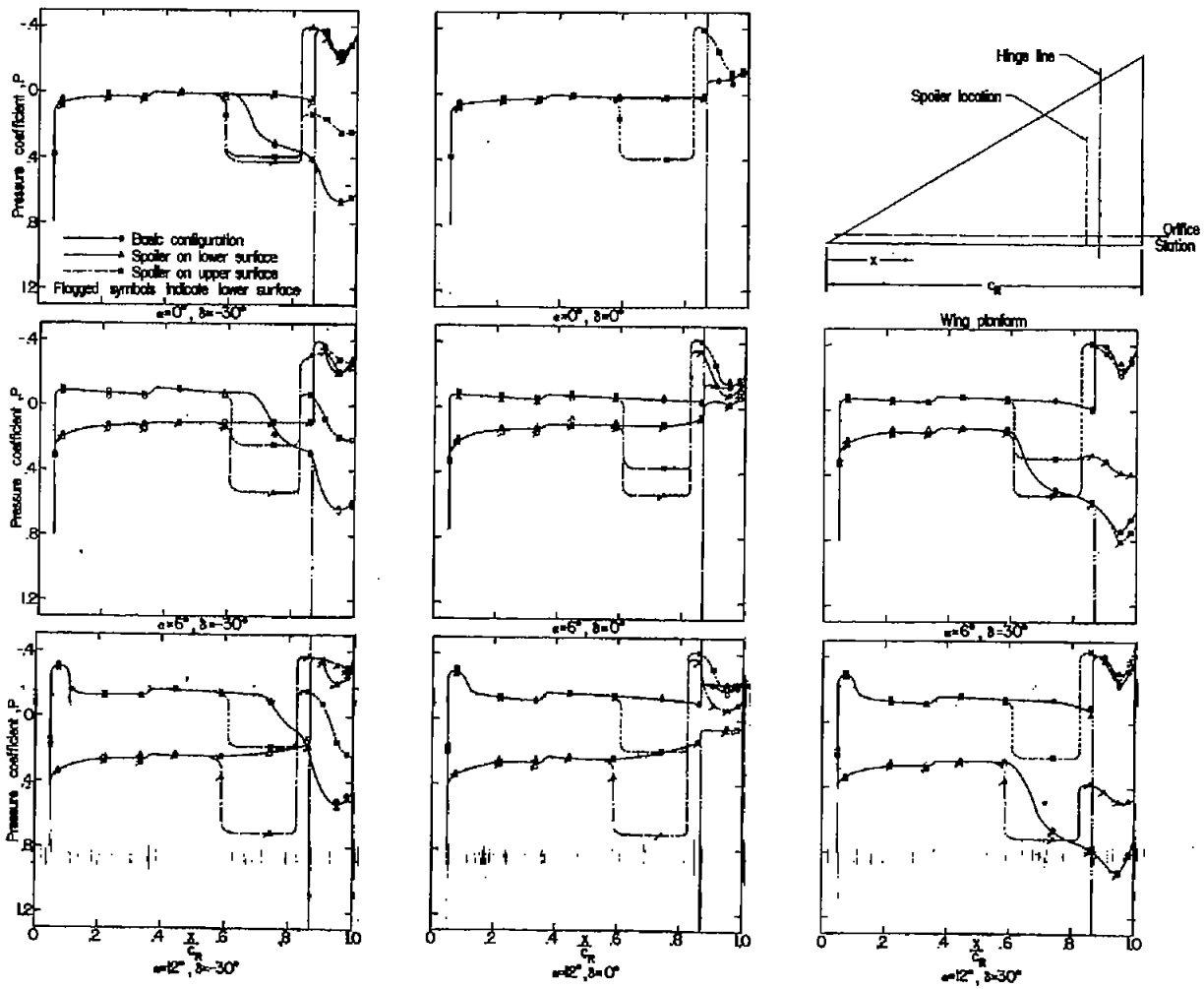

(a) Orifice station 1.

Figure 4.- Illustrative chordwise pressure distributions for the seven spanwise orifice stations.

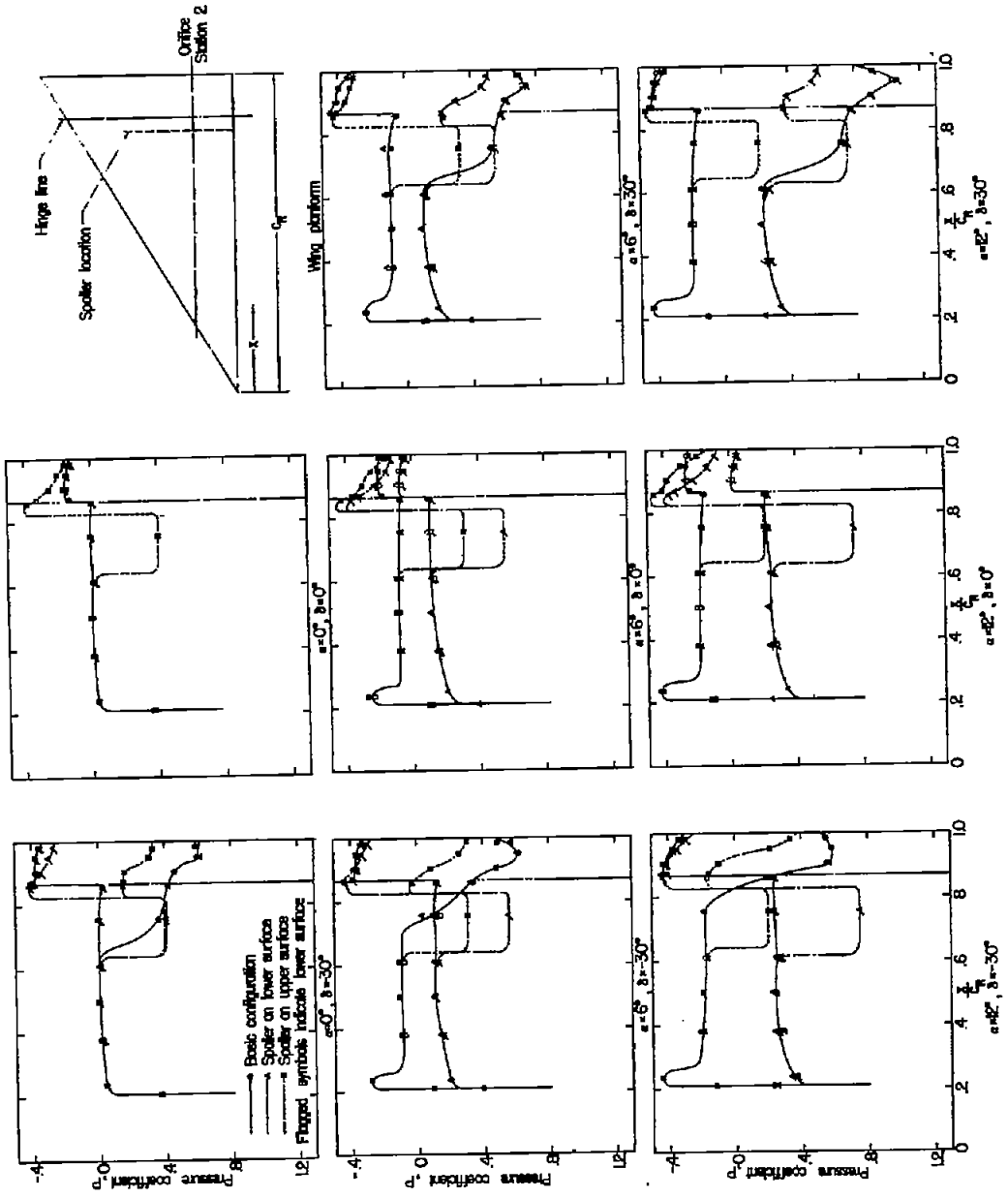

(b) Orifice station 2.

Figure 4.- Continued.

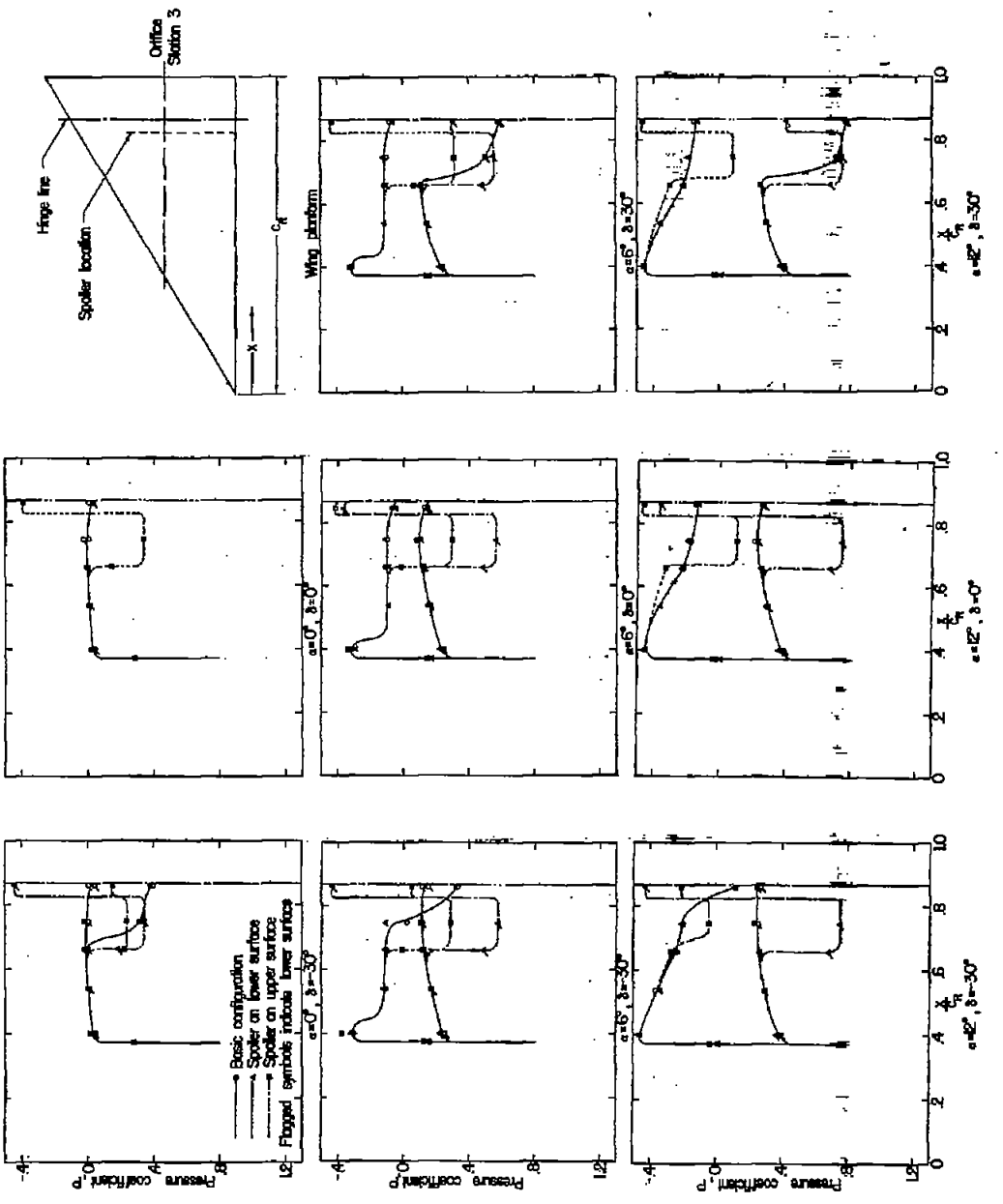

(c) Orifice station 3.

Figure 4.- Continued.

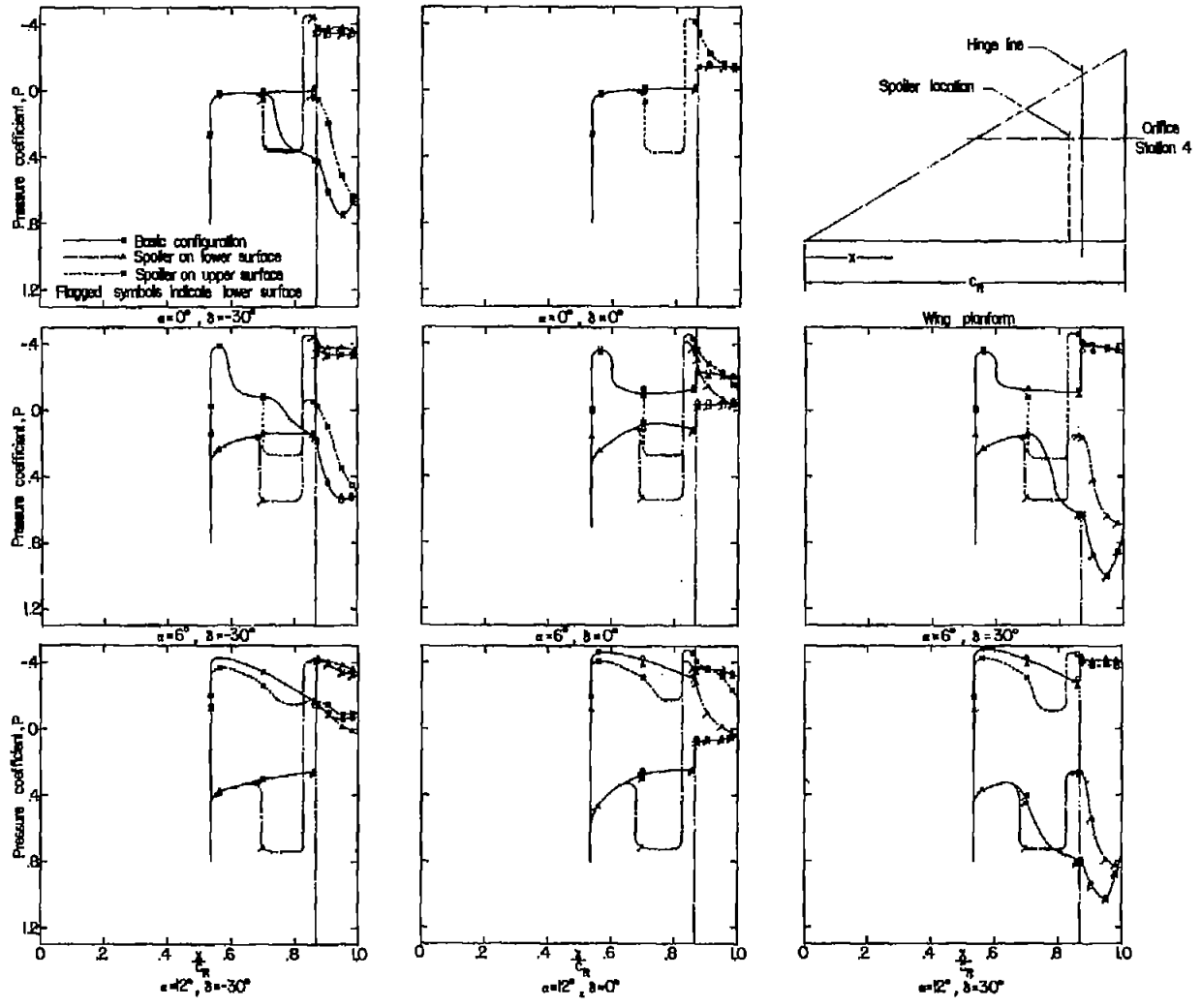

(d) Orifice station 4.

Figure 4.- Continued.

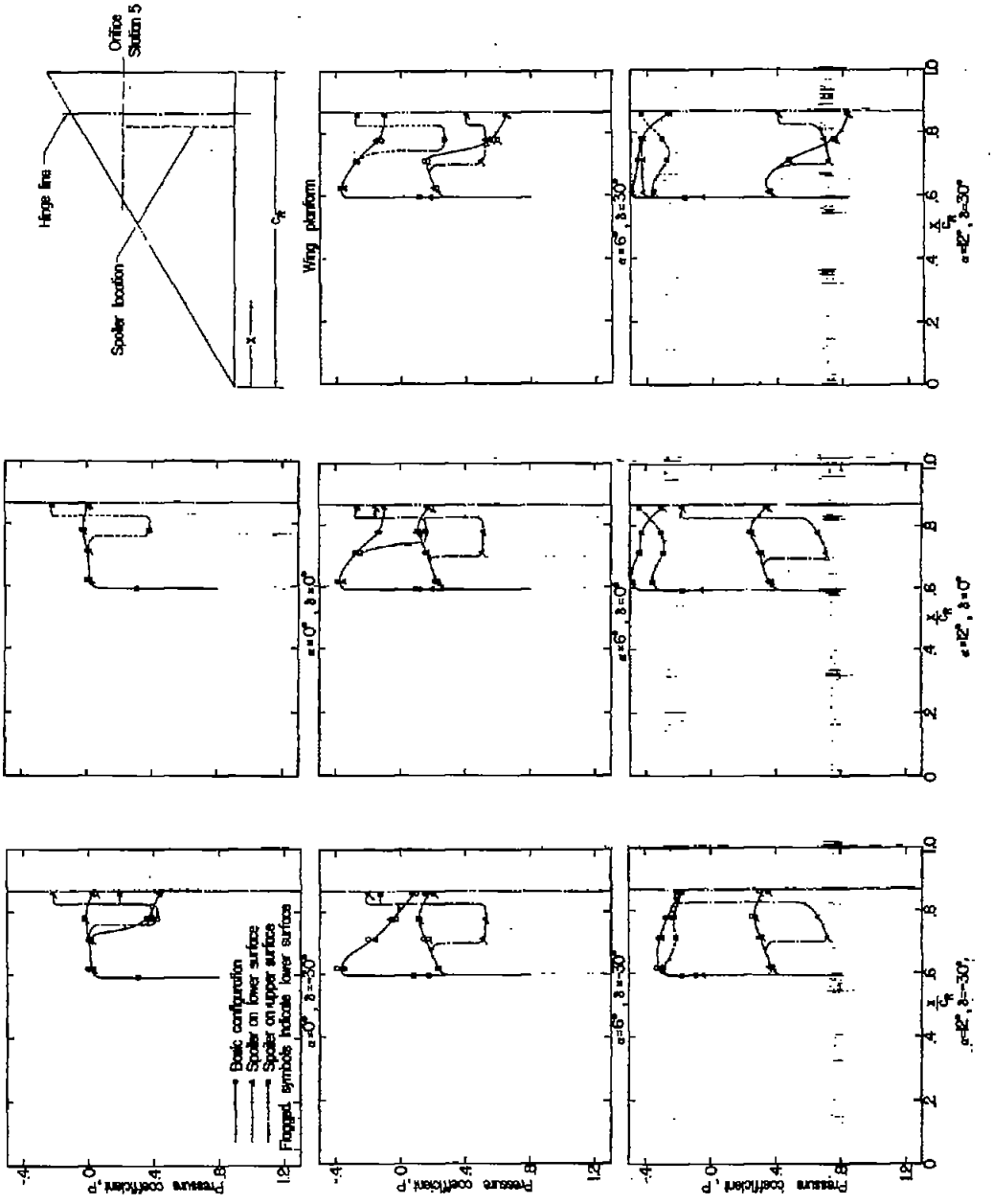

(e) Orifice station 5.

Figure 4.- Continued.

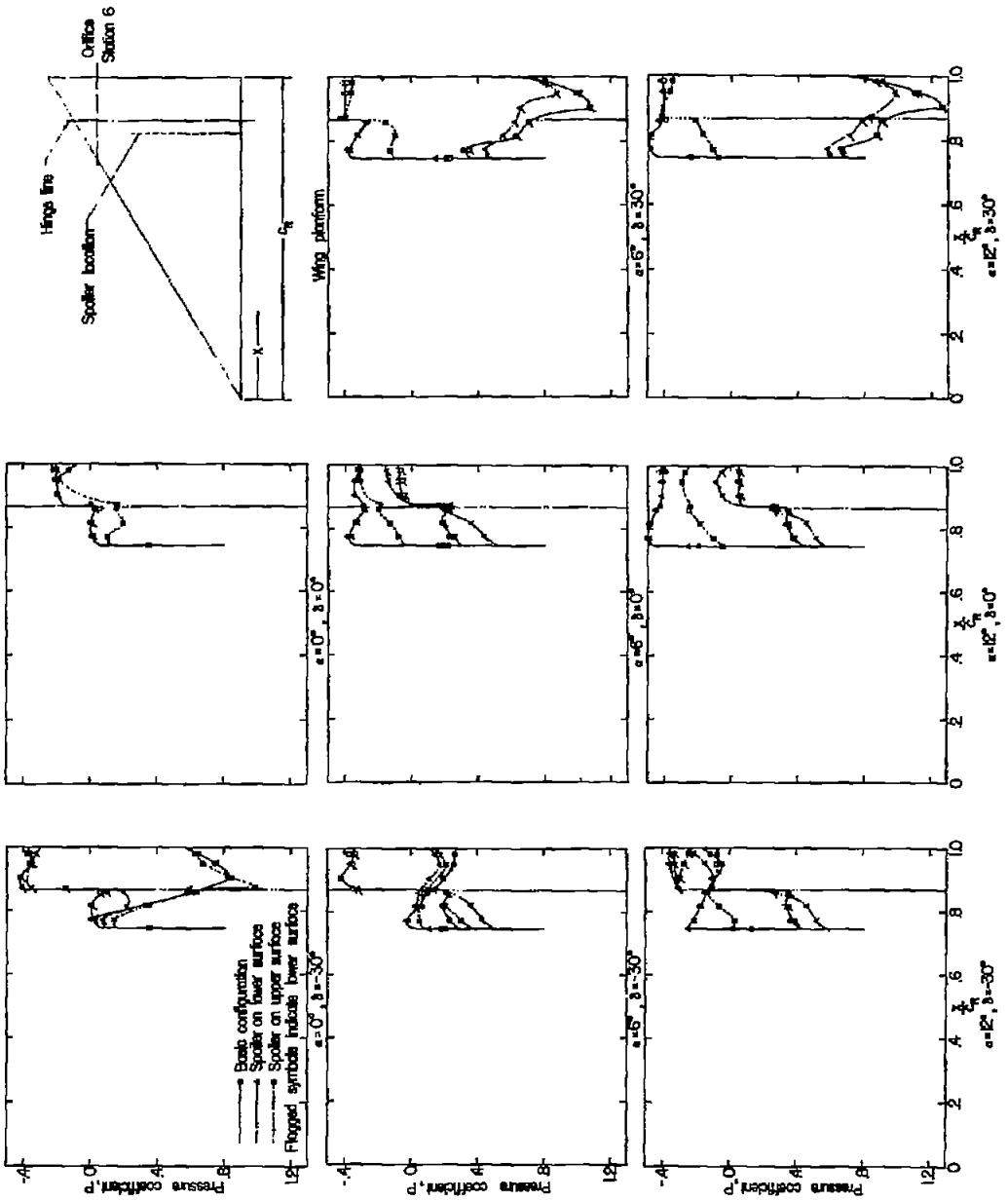

(f) Orifice station 6.

Figure 4.- Continued.

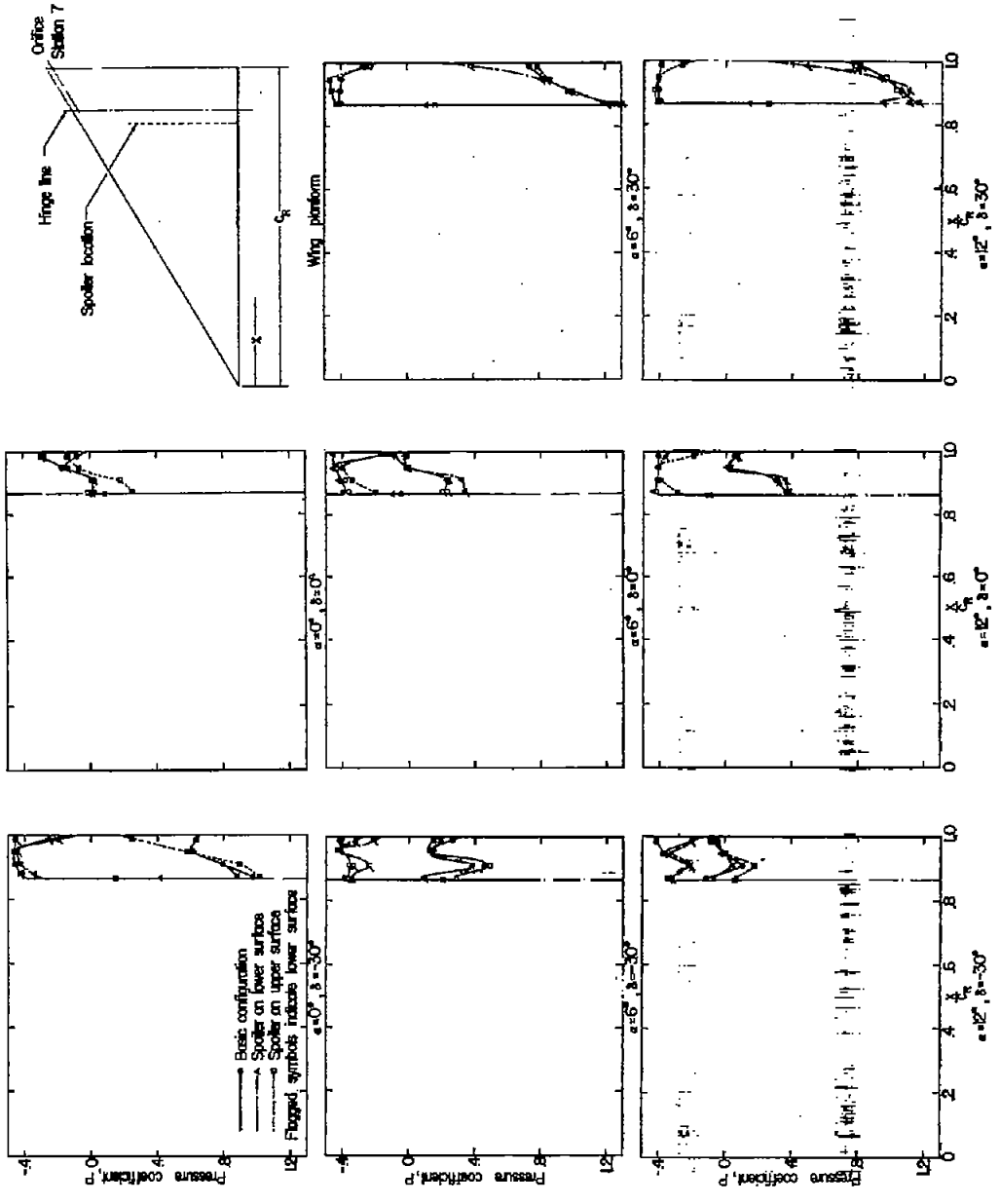

(g) Orifice station 7.

Figure 4.- Concluded.

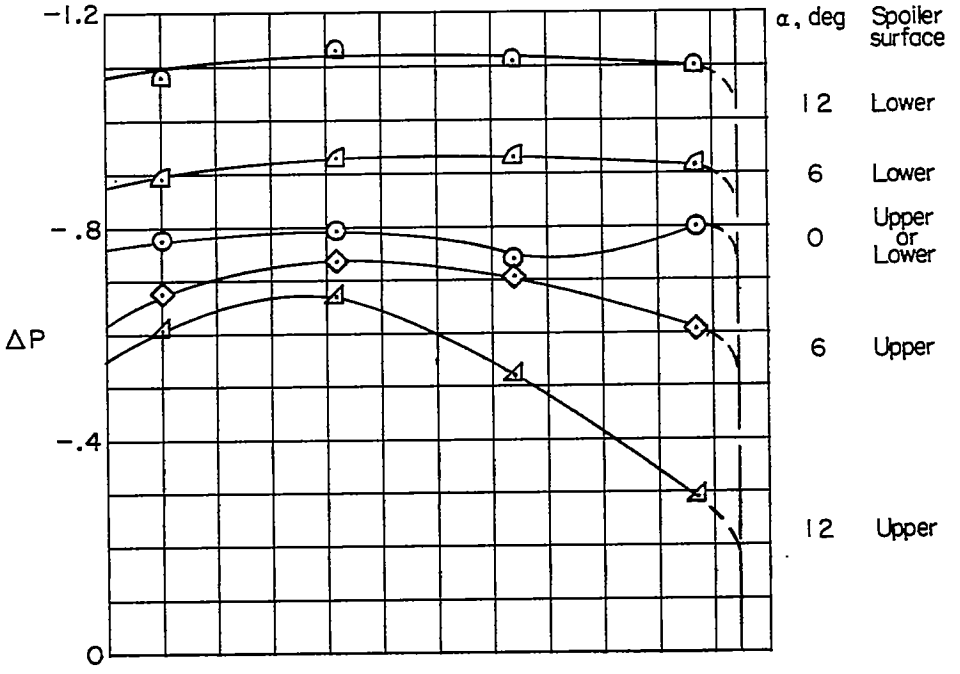

(a) $\delta = 0^{\circ}$.

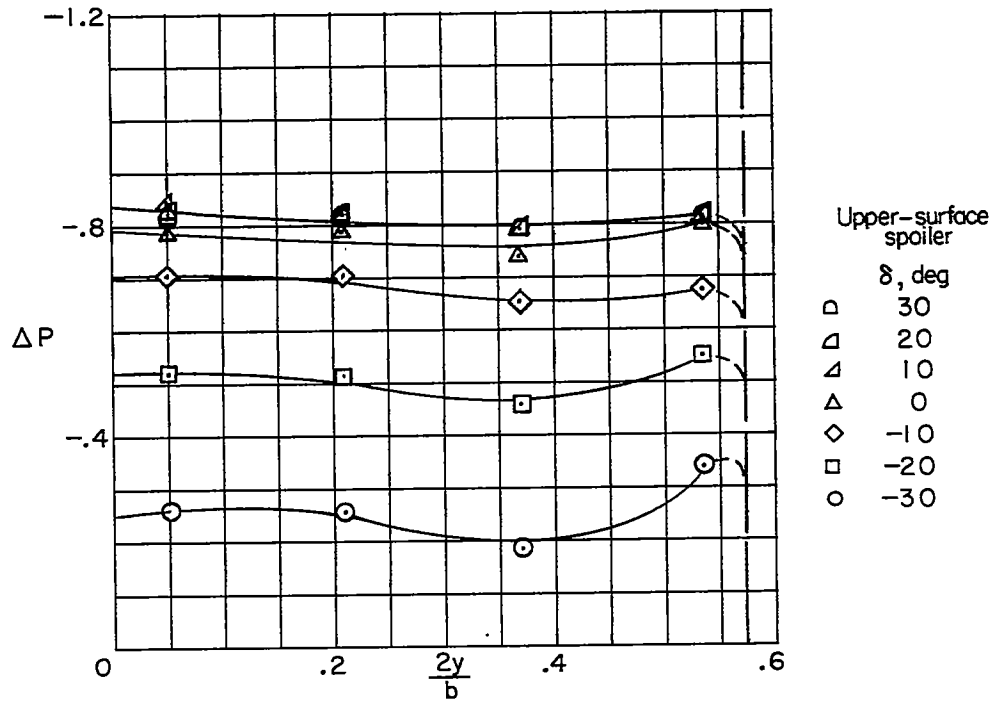

(b) $\alpha = 0^{\circ}$. Upper-surface spoiler.

Figure 5.- Spanwise variation of incremental pressure coefficient on wing surface at the spoiler.

[redacted]

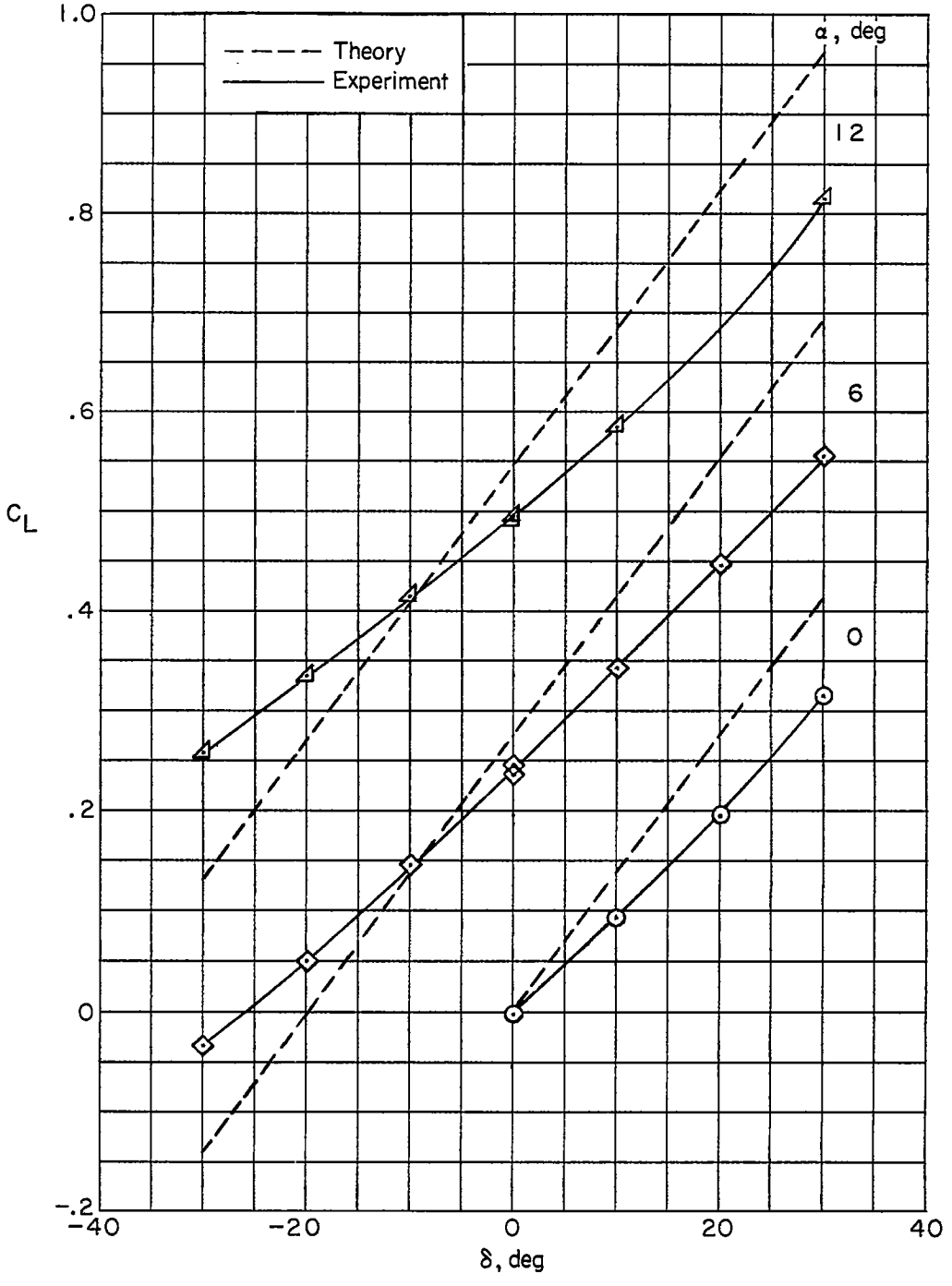

(a) Lift coefficient.

Figure 6.- Variation of semispan-wing lift, root bending-moment, and pitching-moment coefficients with control deflection for basic configuration.

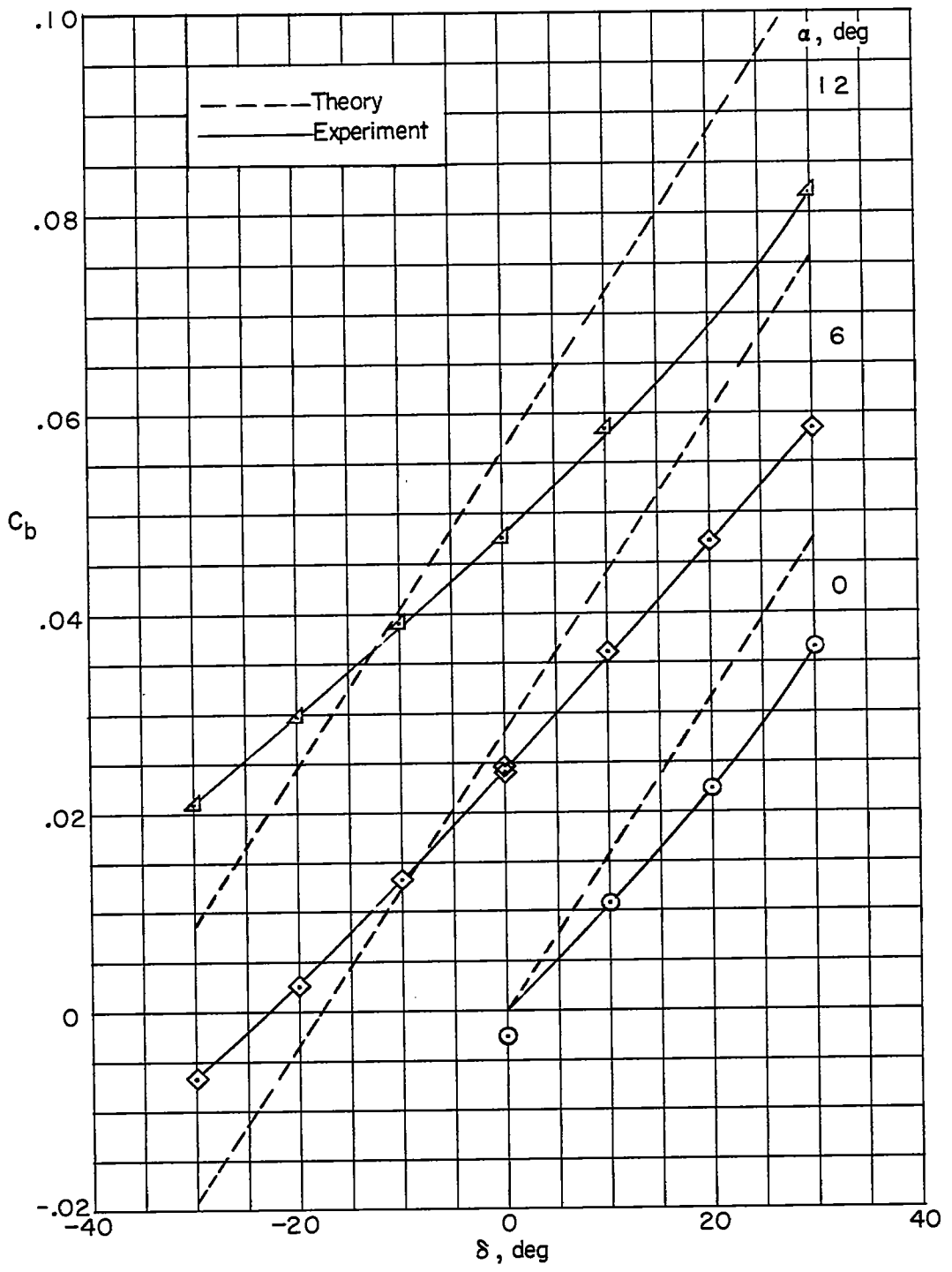

(b) Root bending-moment coefficient.

Figure 6.- Continued.

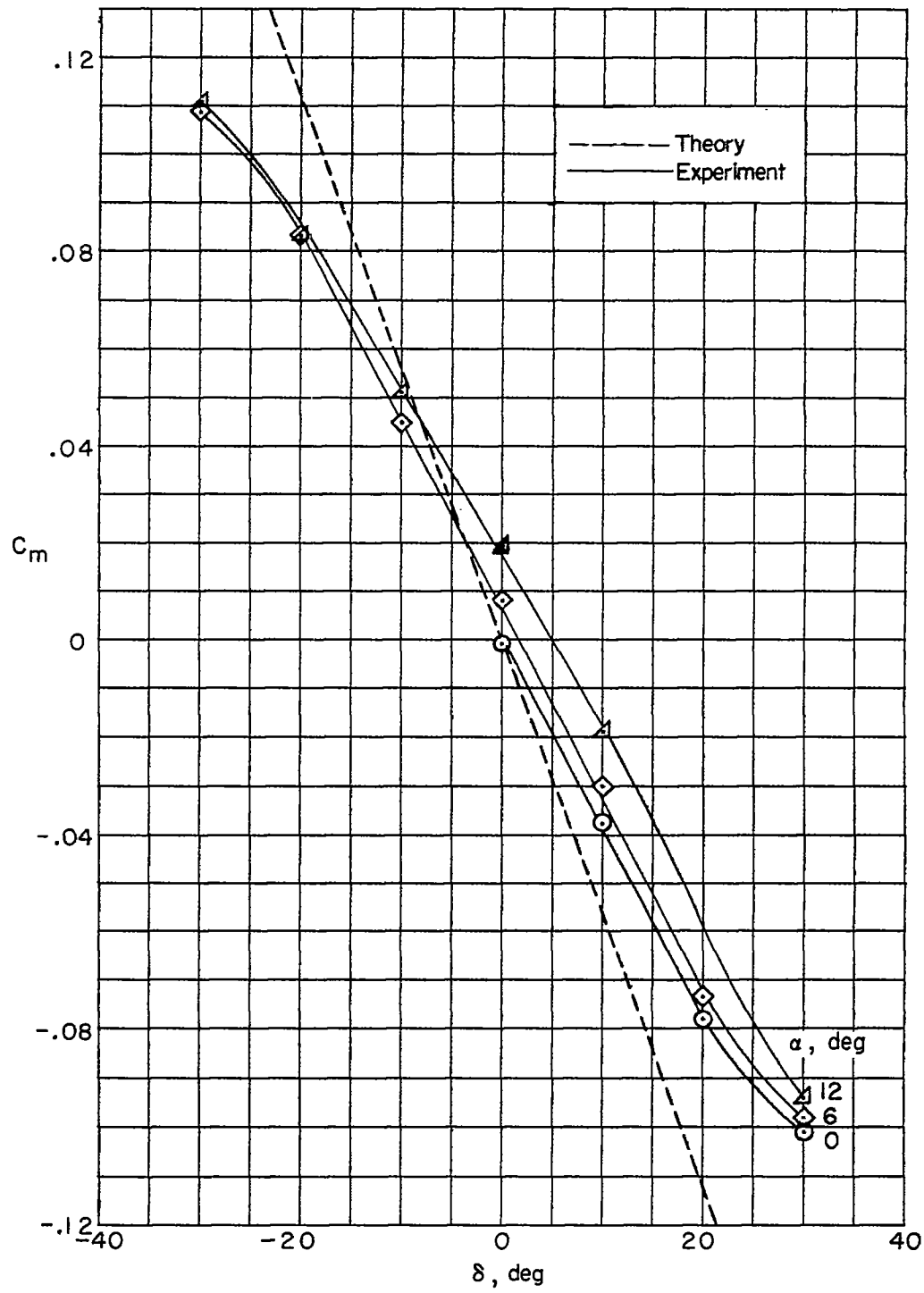

(c) Pitching-moment coefficient.

Figure 6.- Concluded.

[redacted]

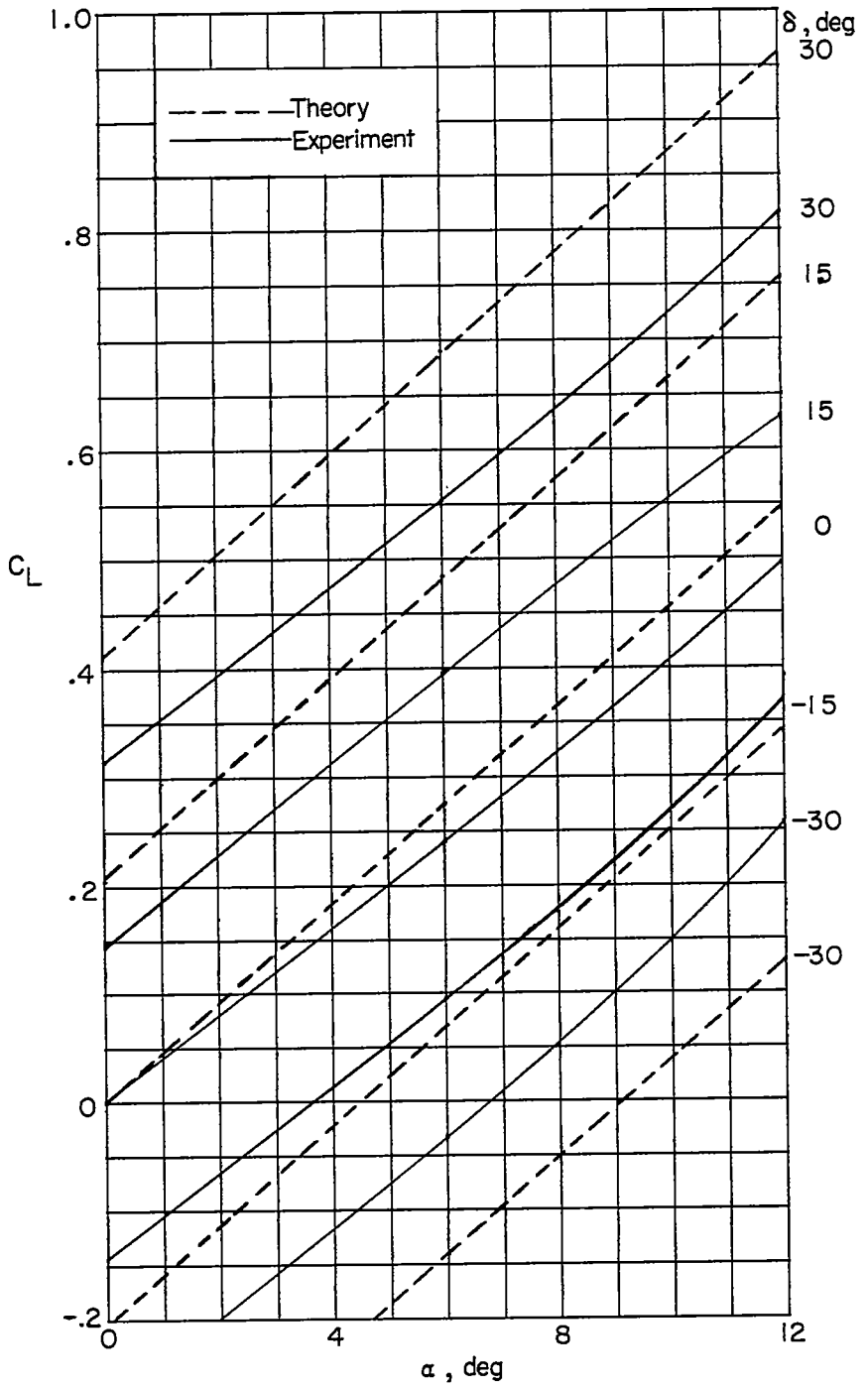

(a) Lift coefficient.

Figure 7.- Variation of semispan-wing lift, root bending-moment, and pitching-moment coefficients with wing angle of attack for basic configuration.

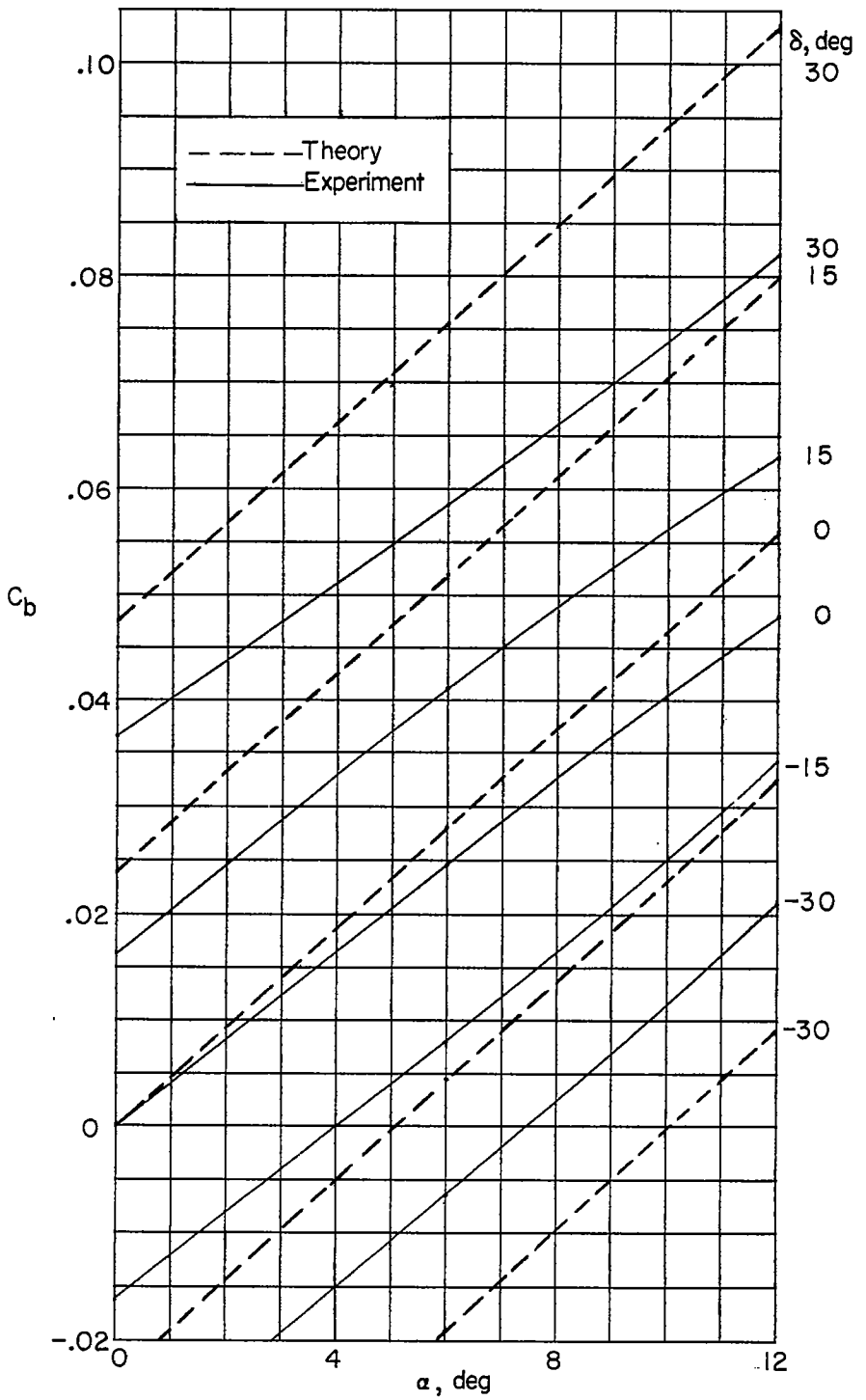

(b) Root bending-moment coefficient.

Figure 7.- Continued.

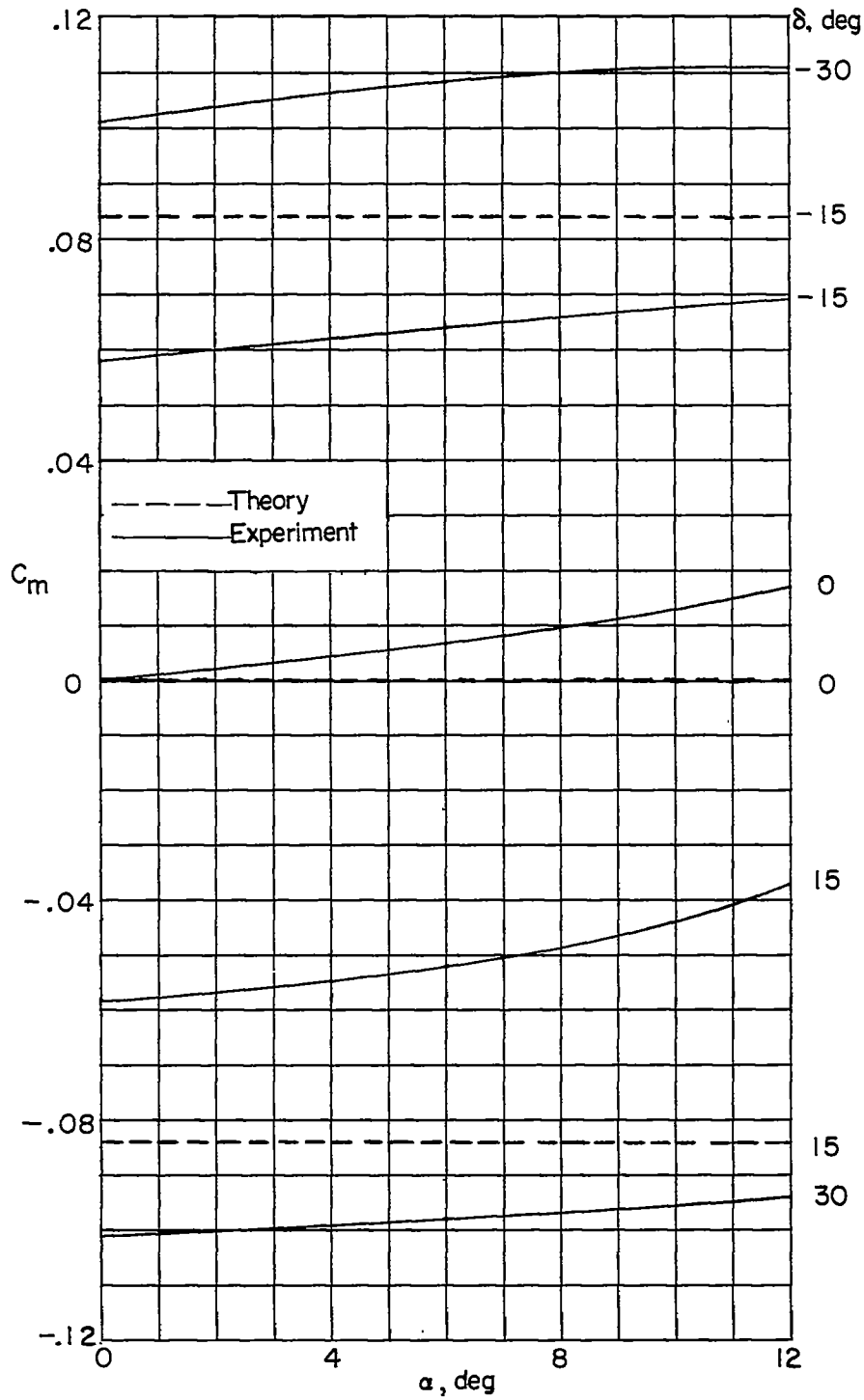

(c) Pitching-moment coefficient.

Figure 7.- Concluded.

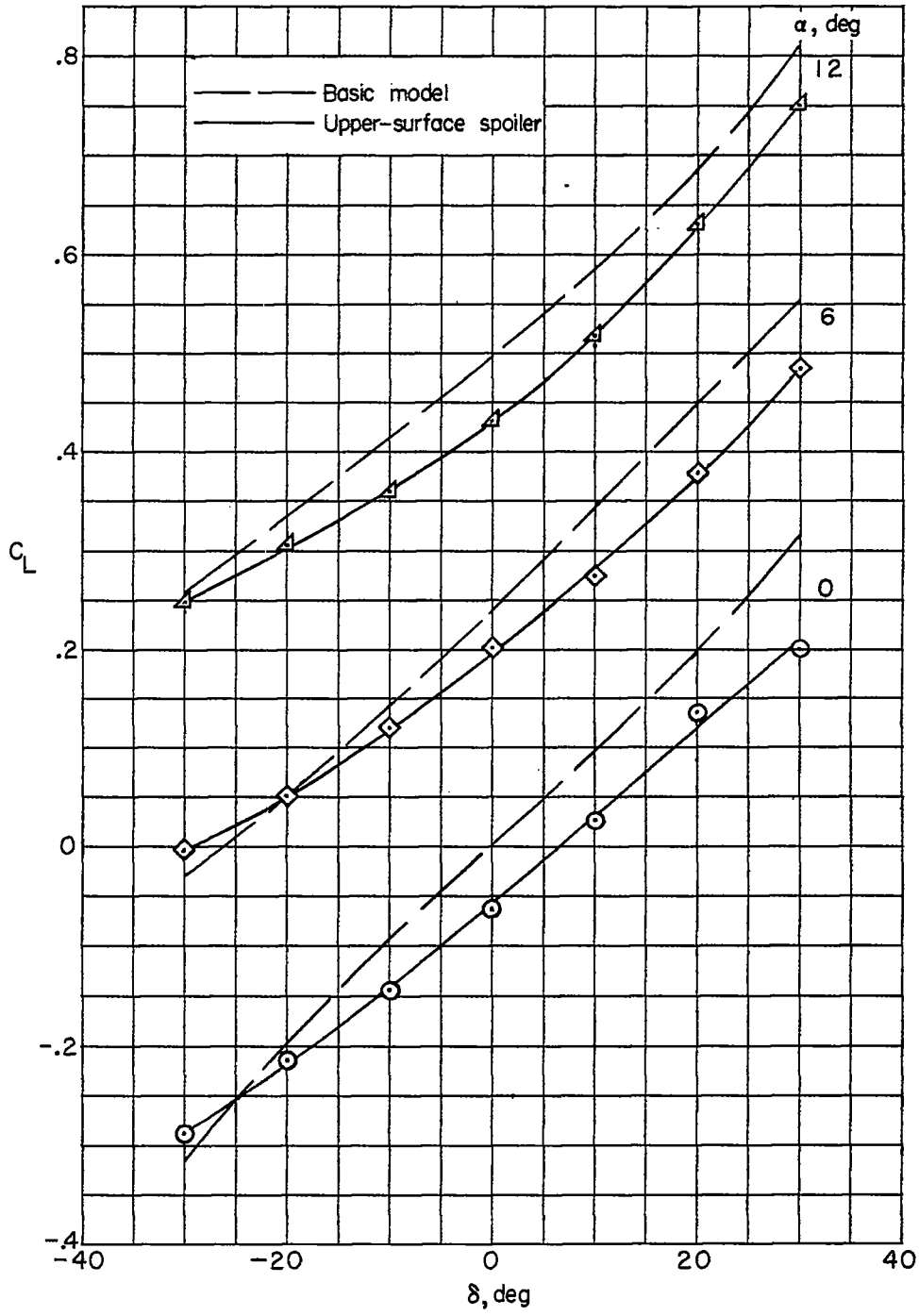

(a) Lift coefficient.

Figure 8.- Variation of semispan-wing lift, root bending-moment, and pitching-moment coefficients with control deflection for the upper-surface spoiler configuration and the basic configuration.

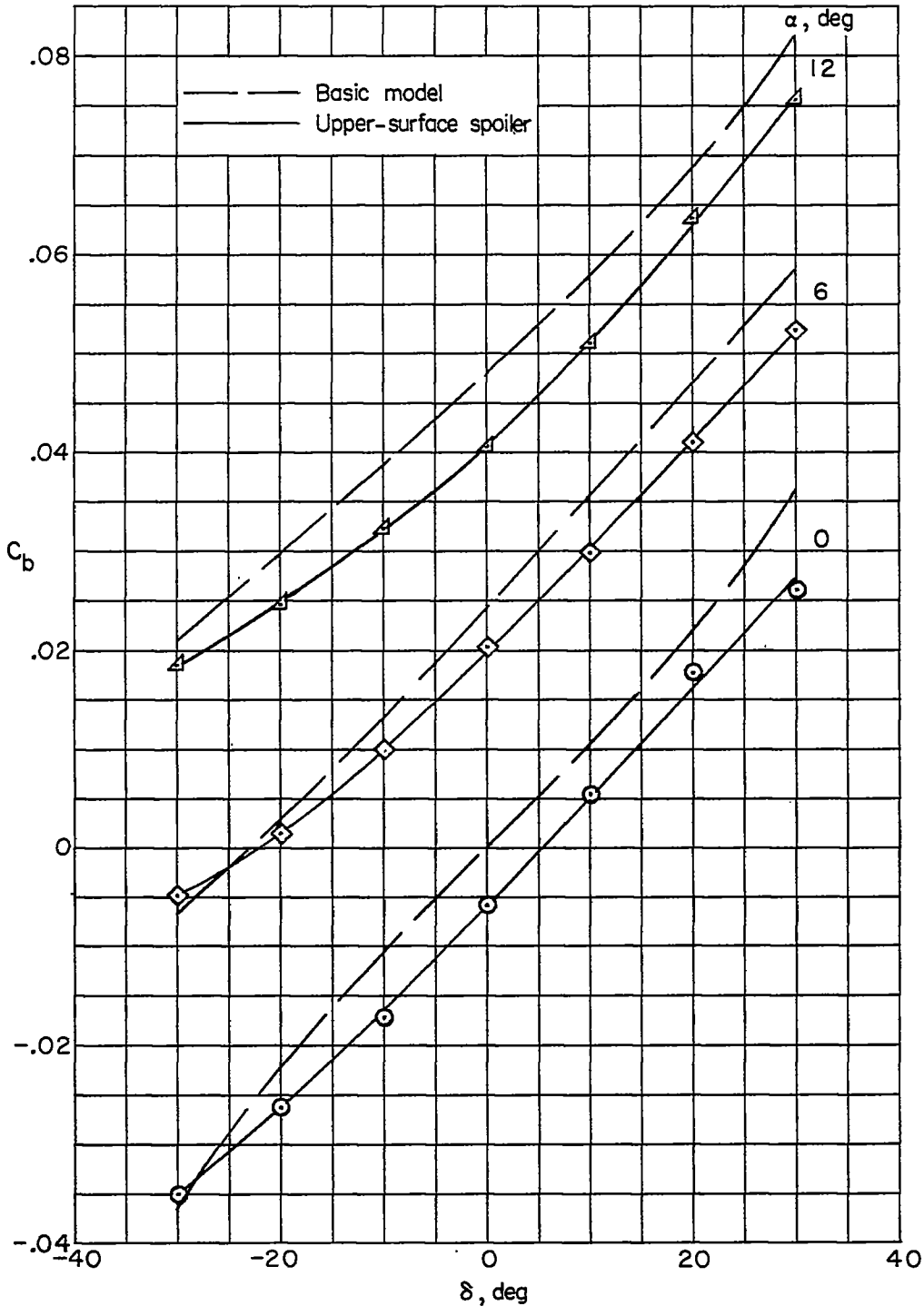

(b) Root bending-moment coefficient.

Figure 8.- Continued.

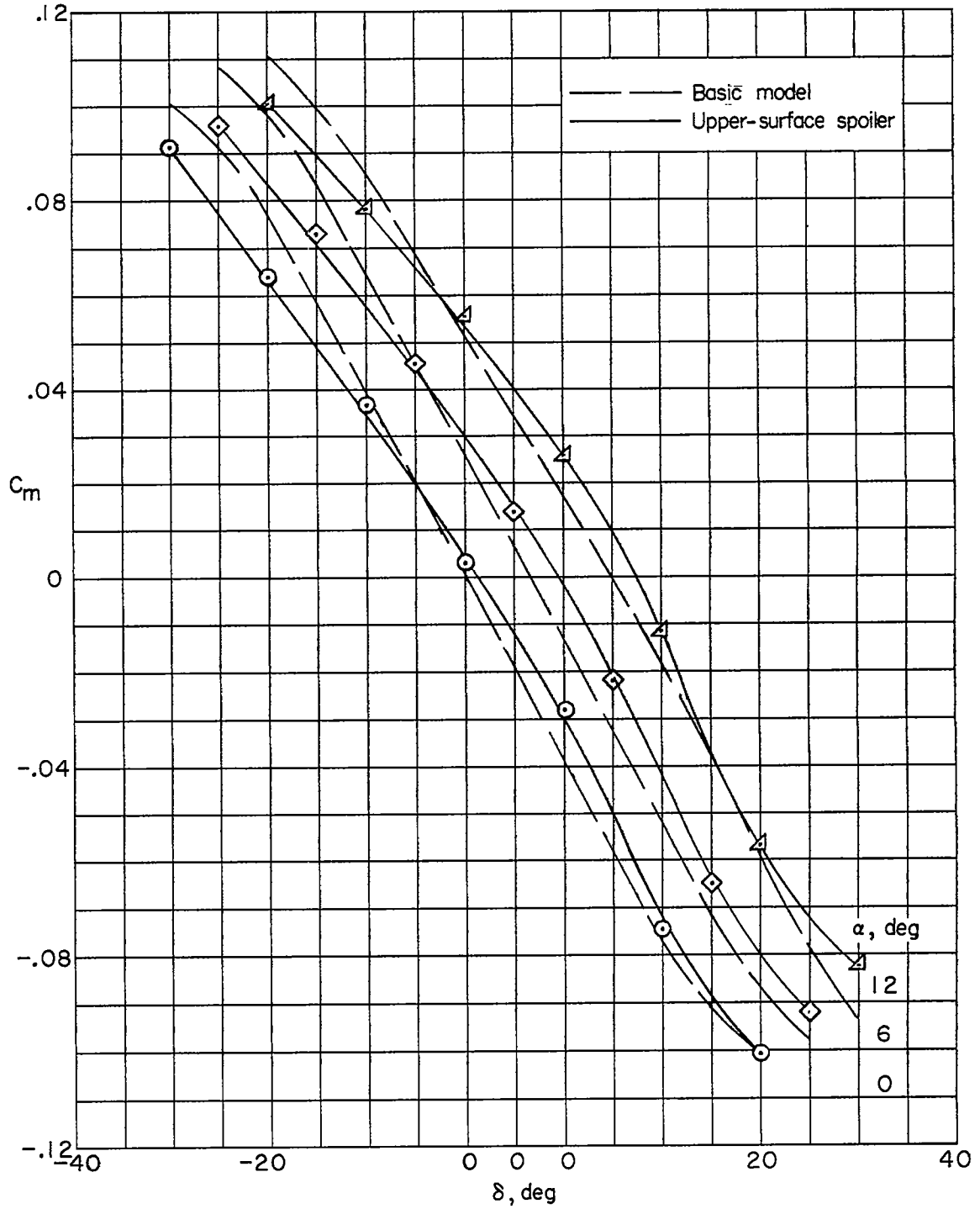

(c) Pitching-moment coefficient.

Figure 8.- Concluded.

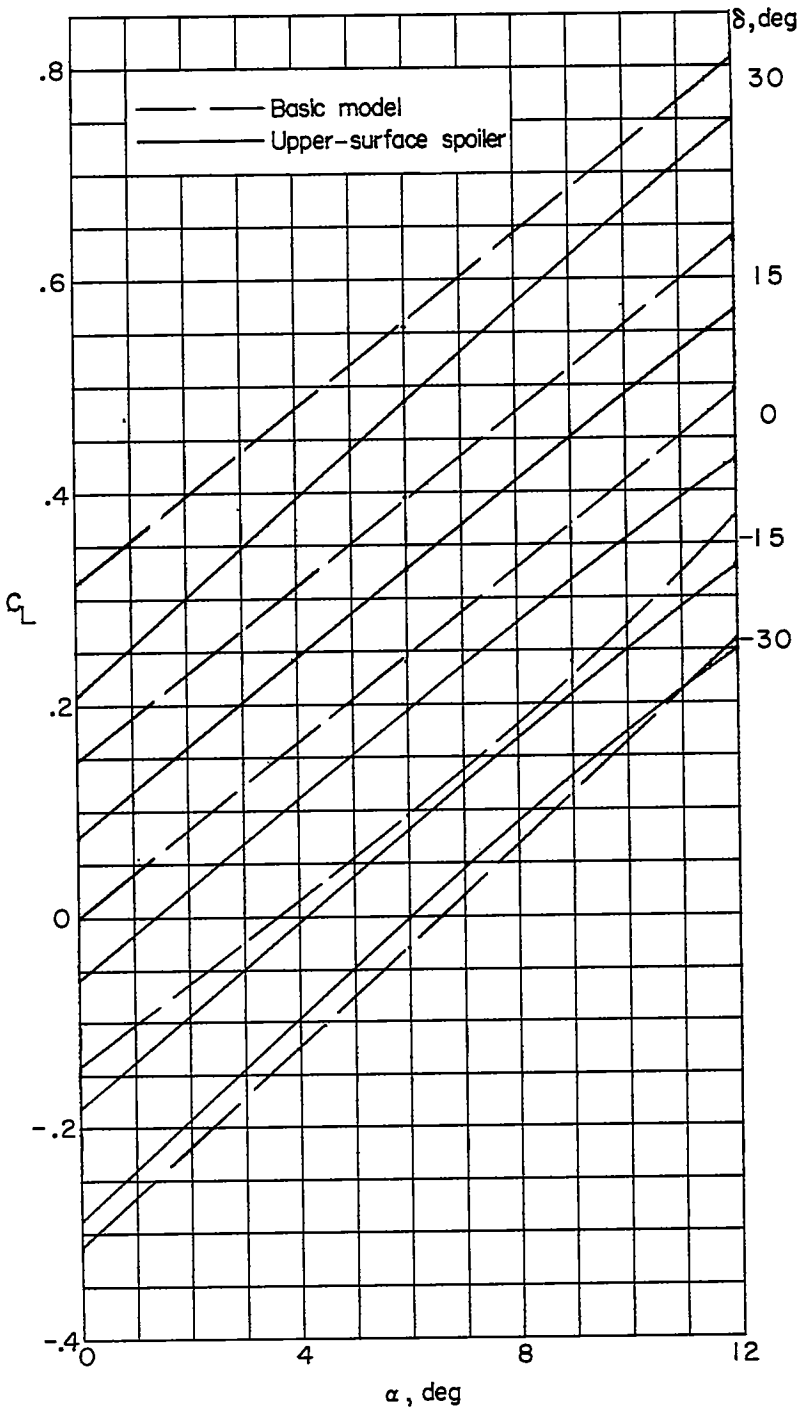

(a) Lift coefficient.

Figure 9.- Variation of semispan-wing lift, root bending-moment, and pitching-moment coefficients with wing angle of attack for the upper-surface spoiler configuration and the basic configuration.

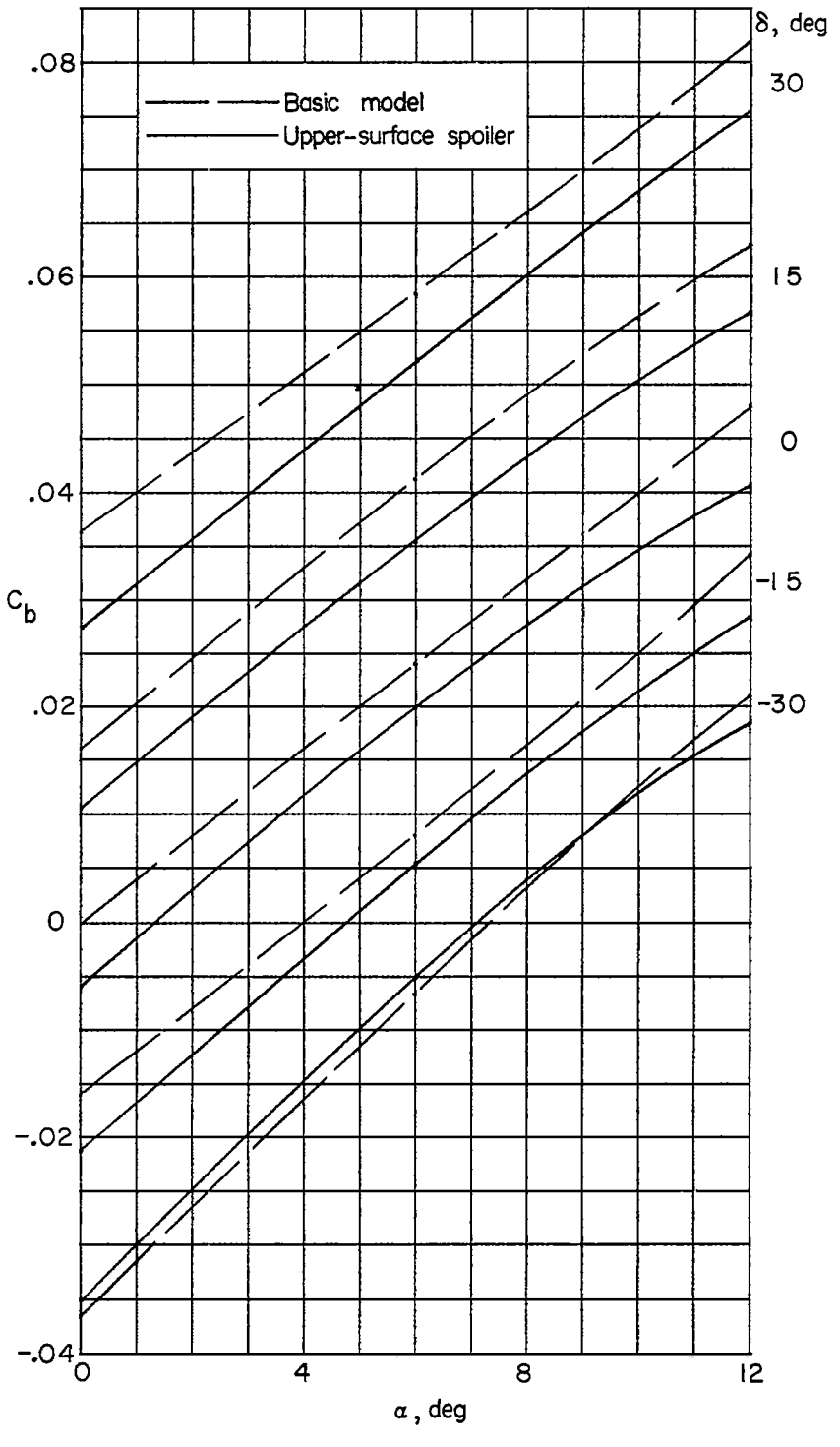

(b) Root bending-moment coefficient.

Figure 9.- Continued.

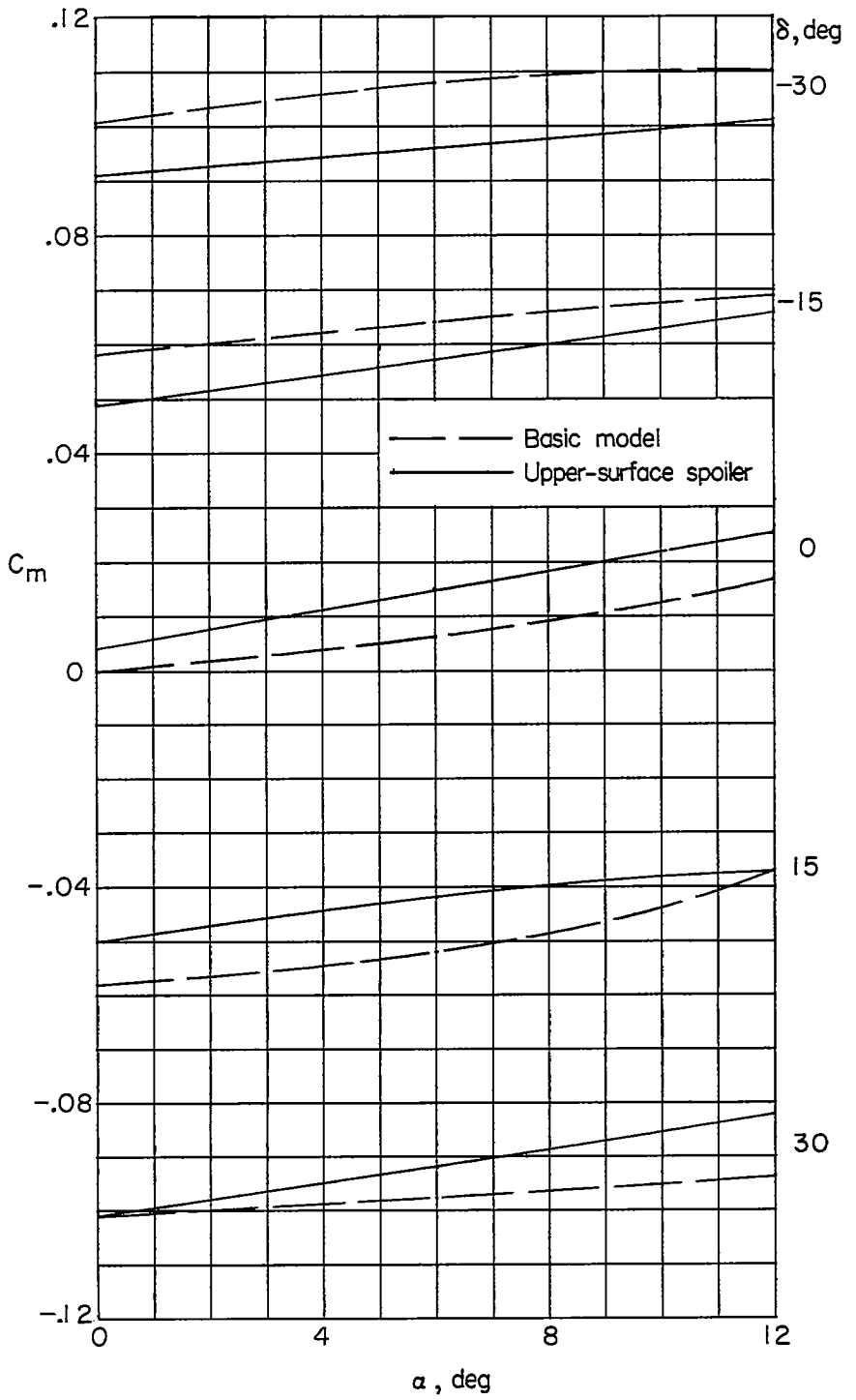

(c) Pitching-moment coefficient.

Figure 9.- Concluded.

[redacted]

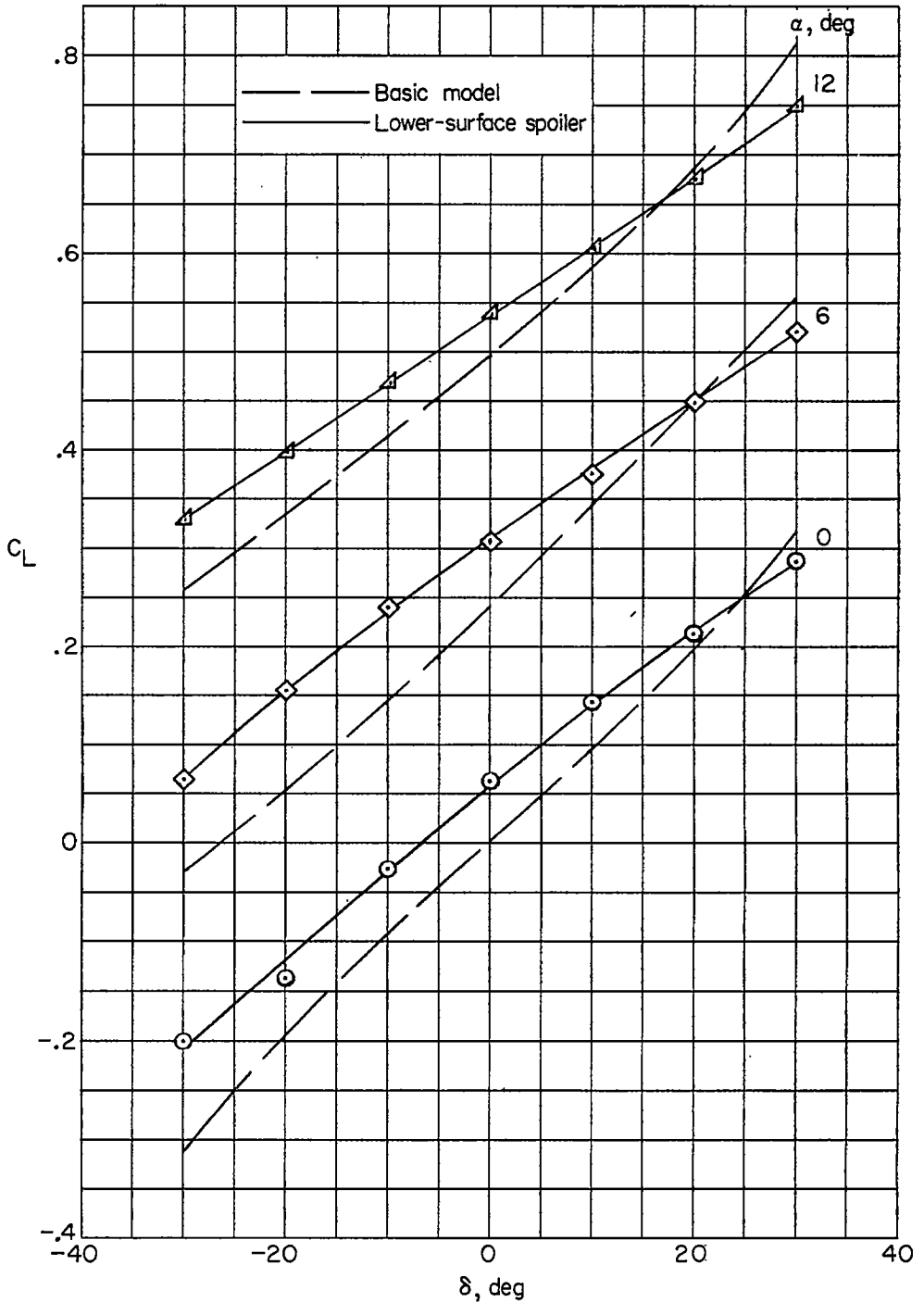

(a) Lift coefficient.

Figure 10.- Variation of semispan-wing lift, root bending-moment, and pitching-moment coefficients with control deflection for the lower-surface spoiler configuration and the basic configuration.

[redacted]

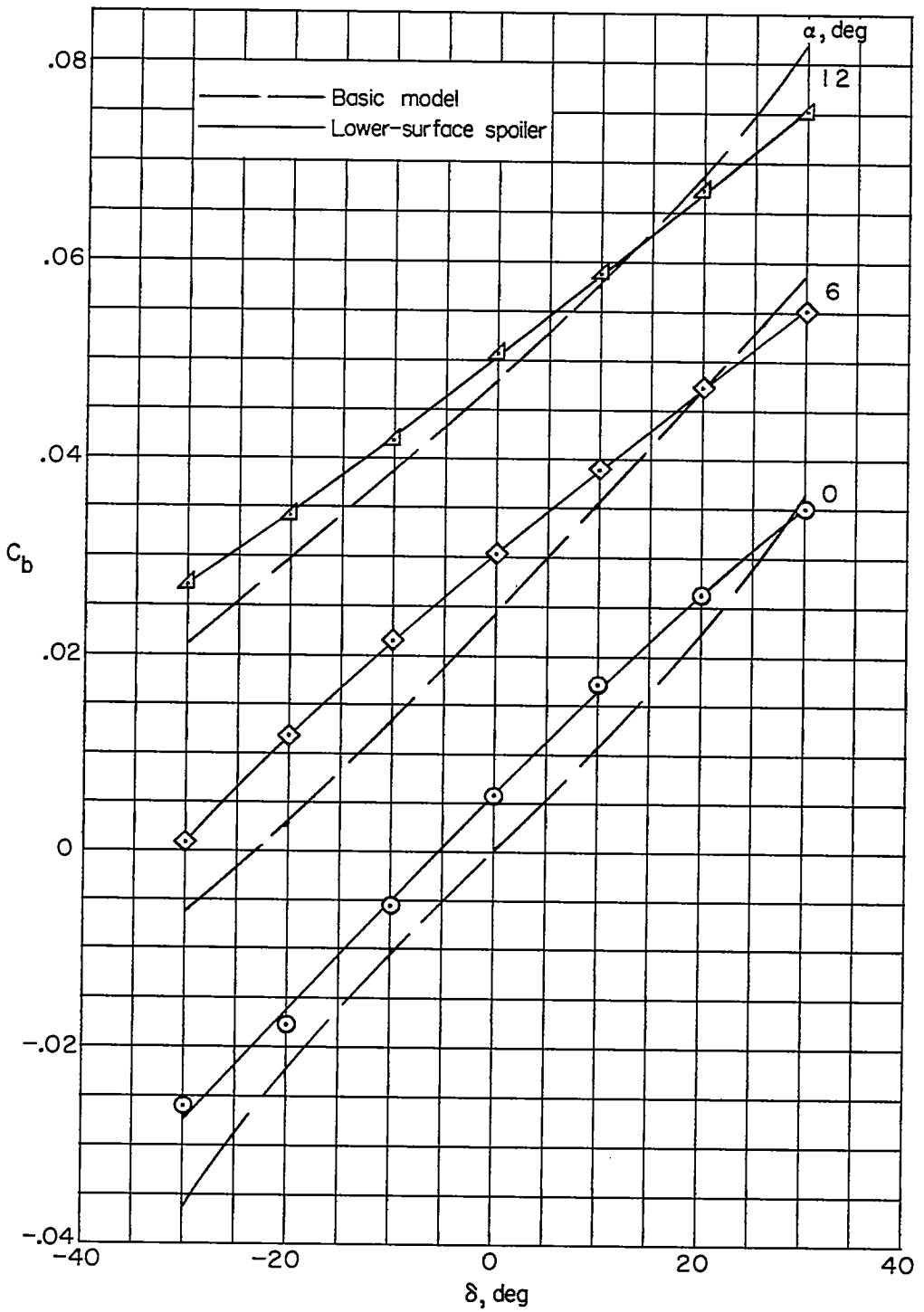

(b) Root bending-moment coefficient.

Figure 10.- Continued.

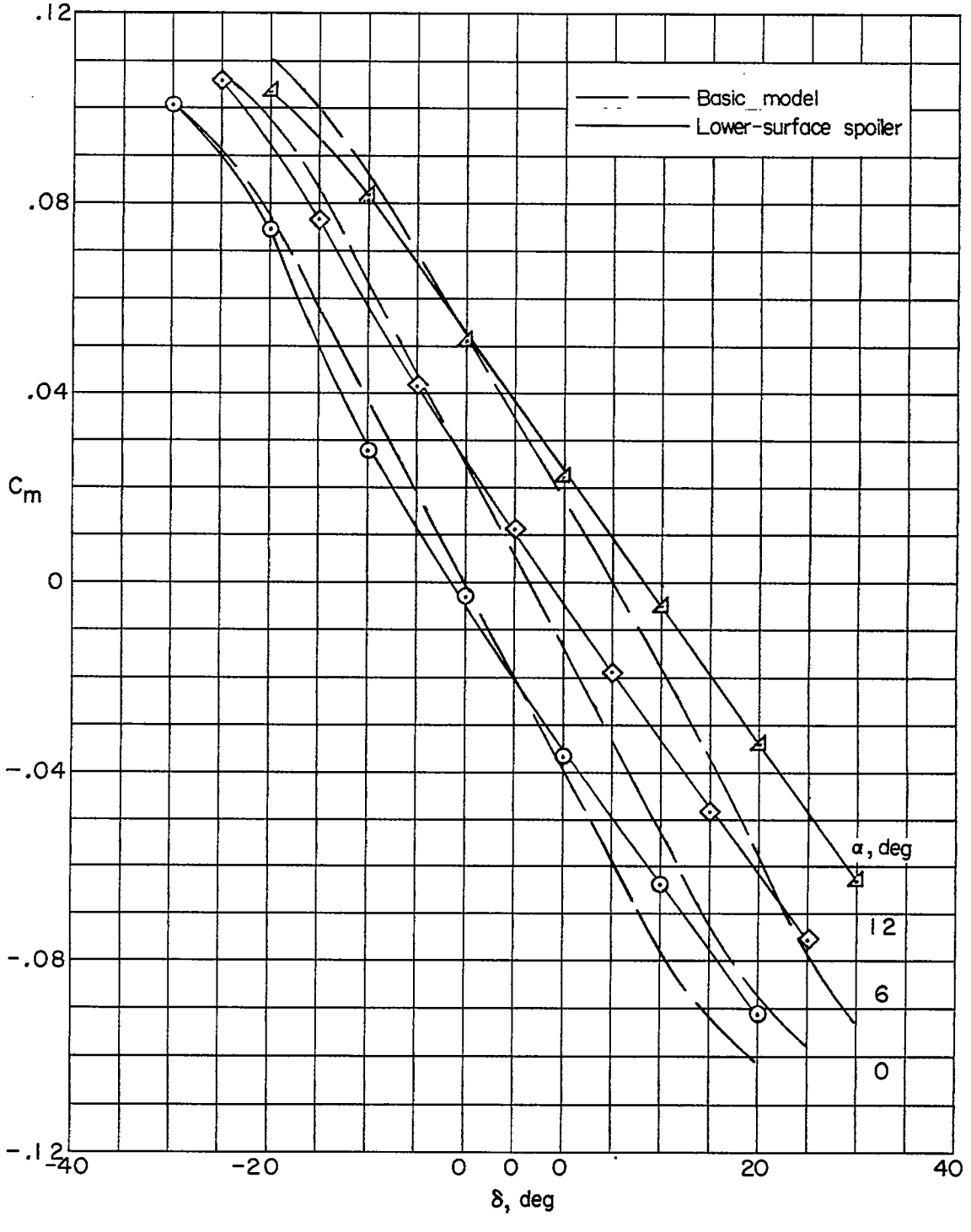

(c) Pitching-moment coefficient.

Figure 10.- Concluded.

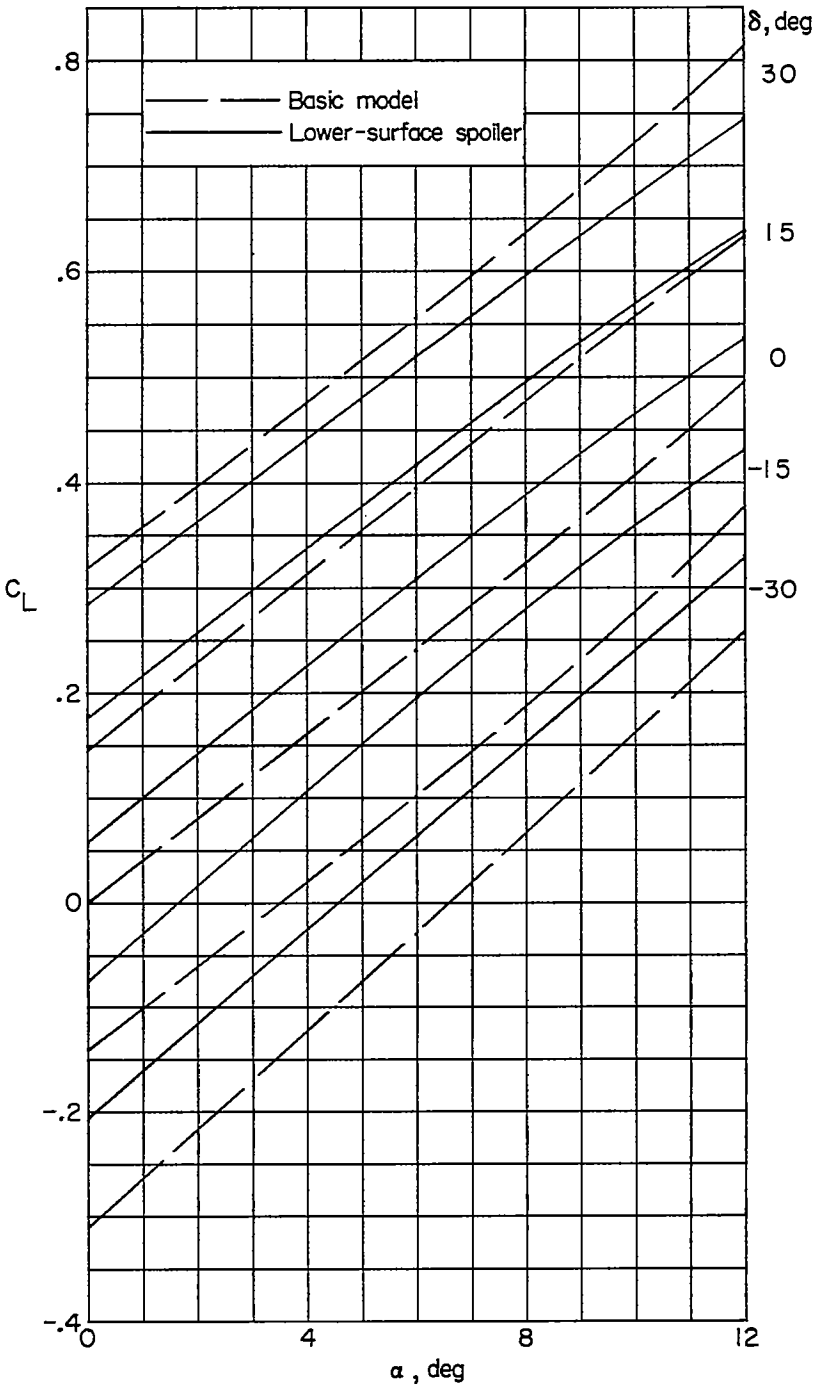

(a) Lift coefficient.

Figure 11.- Variation of semispan-wing lift, root bending-moment, and pitching-moment coefficients with angle of attack for the lower-surface spoiler configuration and the basic configuration.

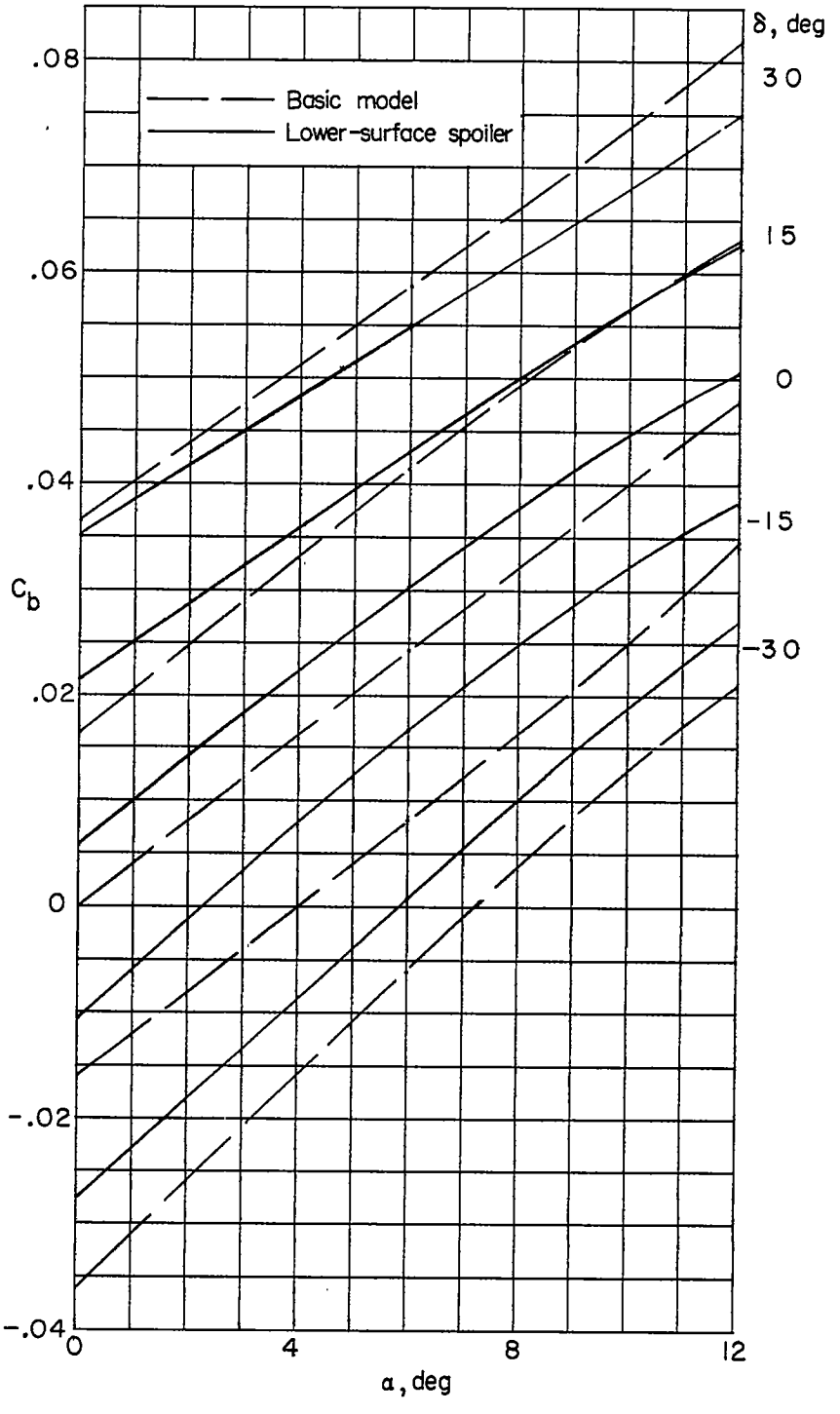

(b) Root bending-moment coefficient.

Figure 11.- Continued.

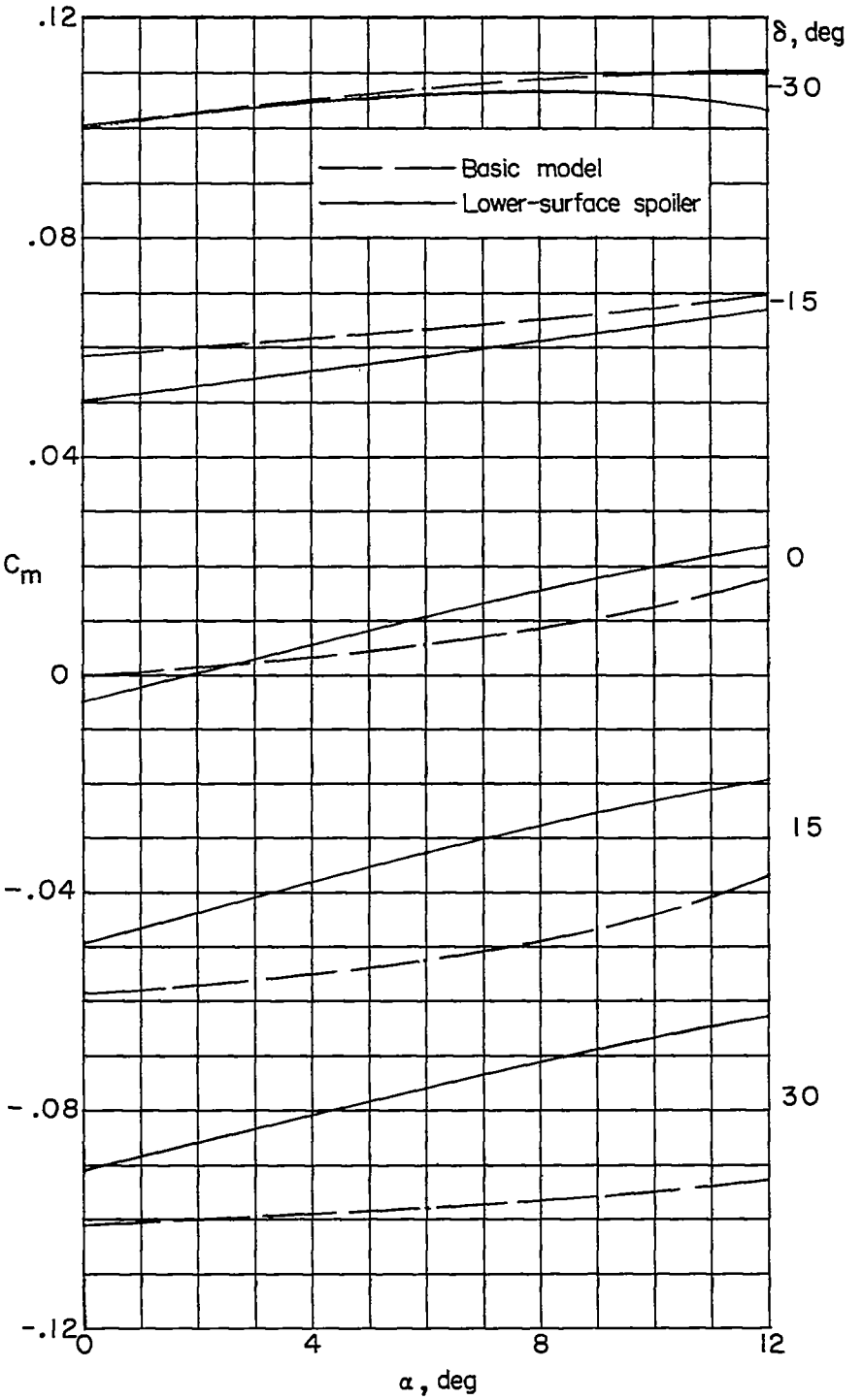

(c) Pitching-moment coefficient.

Figure 11.- Concluded.

[redacted]

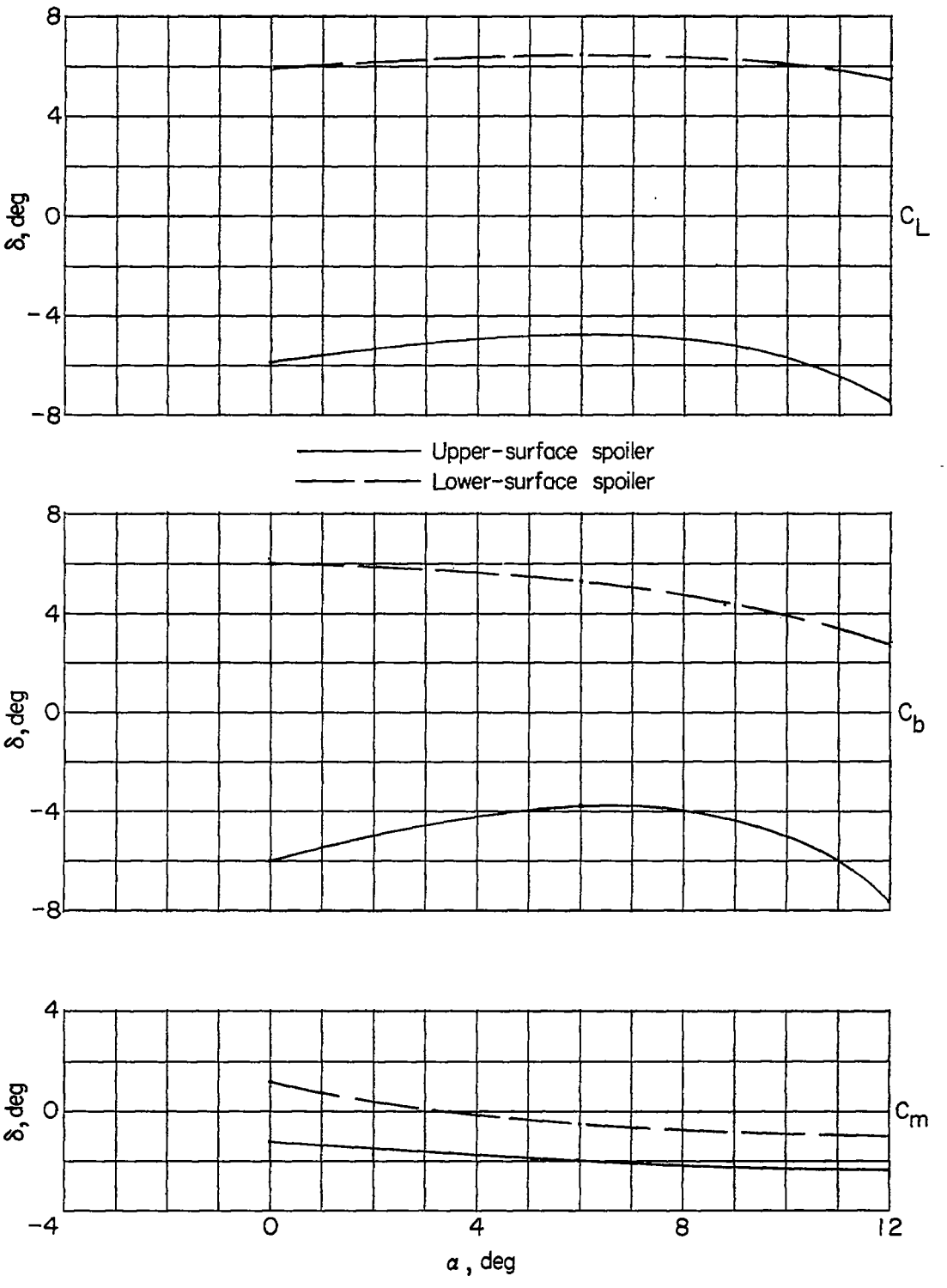

Figure 12.- Control deflection required on basic configuration to produce the effectiveness provided by spoilers alone.

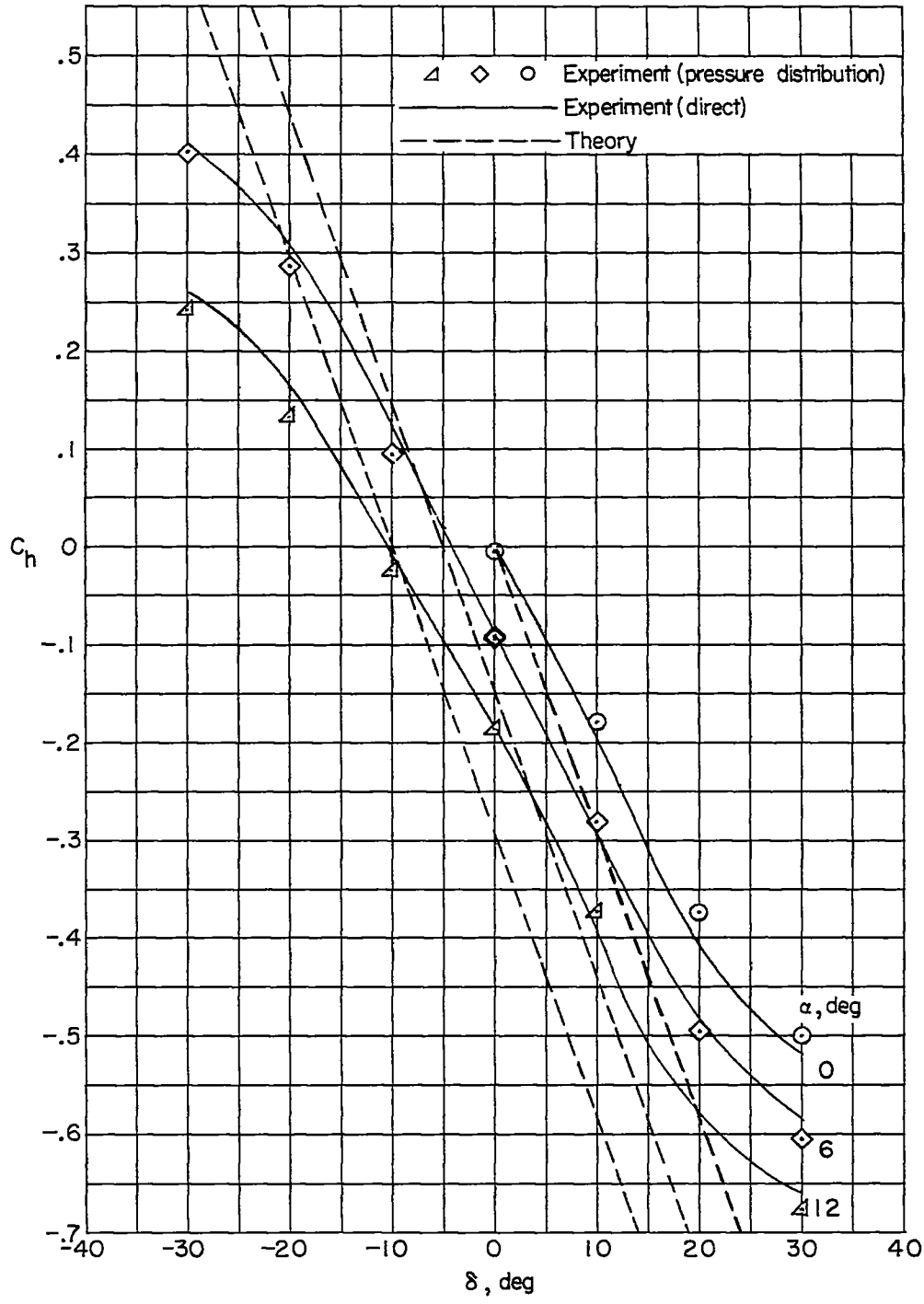

(a) C_h against δ.

Figure 13.- Variation of control hinge-moment coefficient with control deflection and wing angle of attack for the basic configuration.

[redacted]

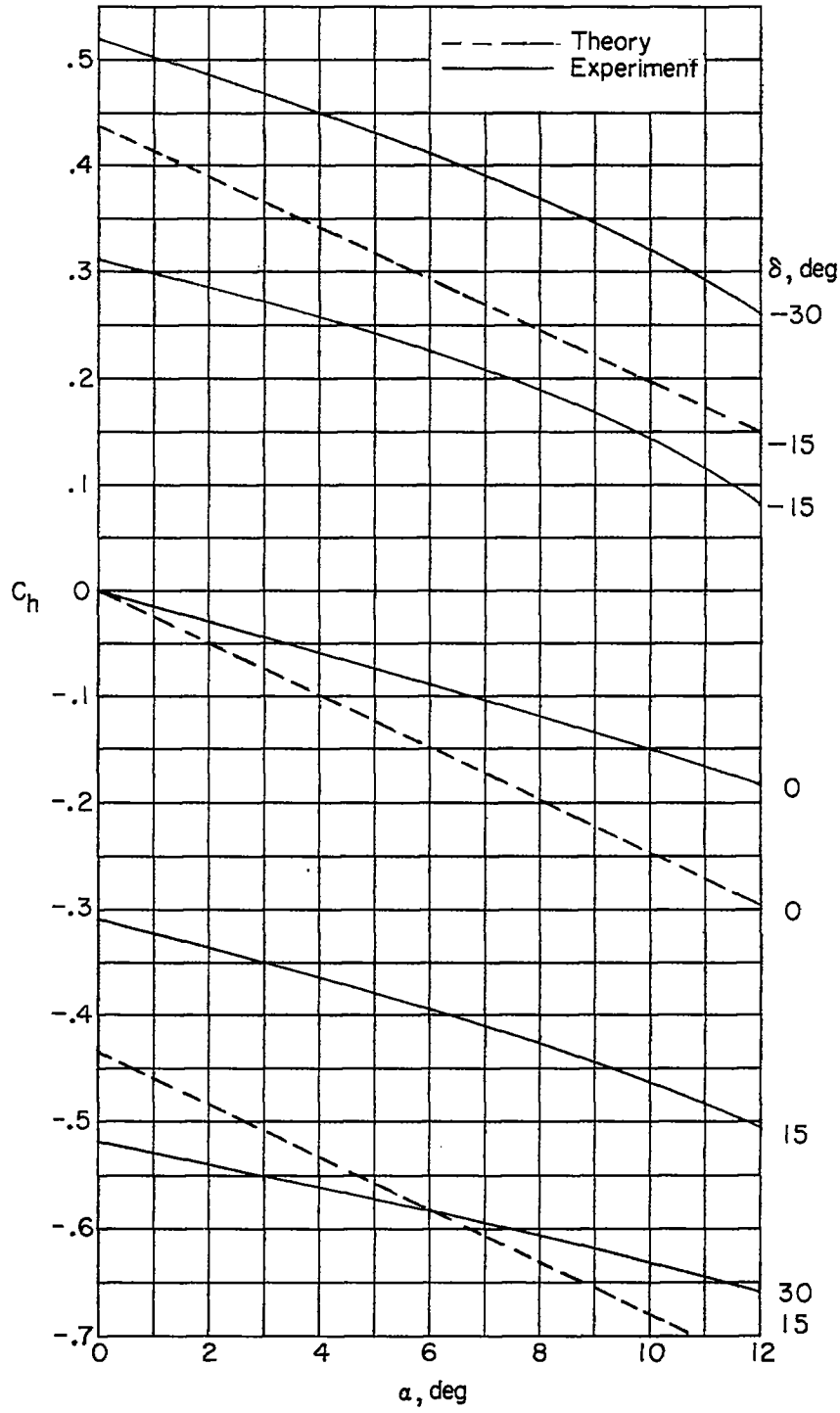

(b) C_h against α.

Figure 13.- Concluded.

[redacted]

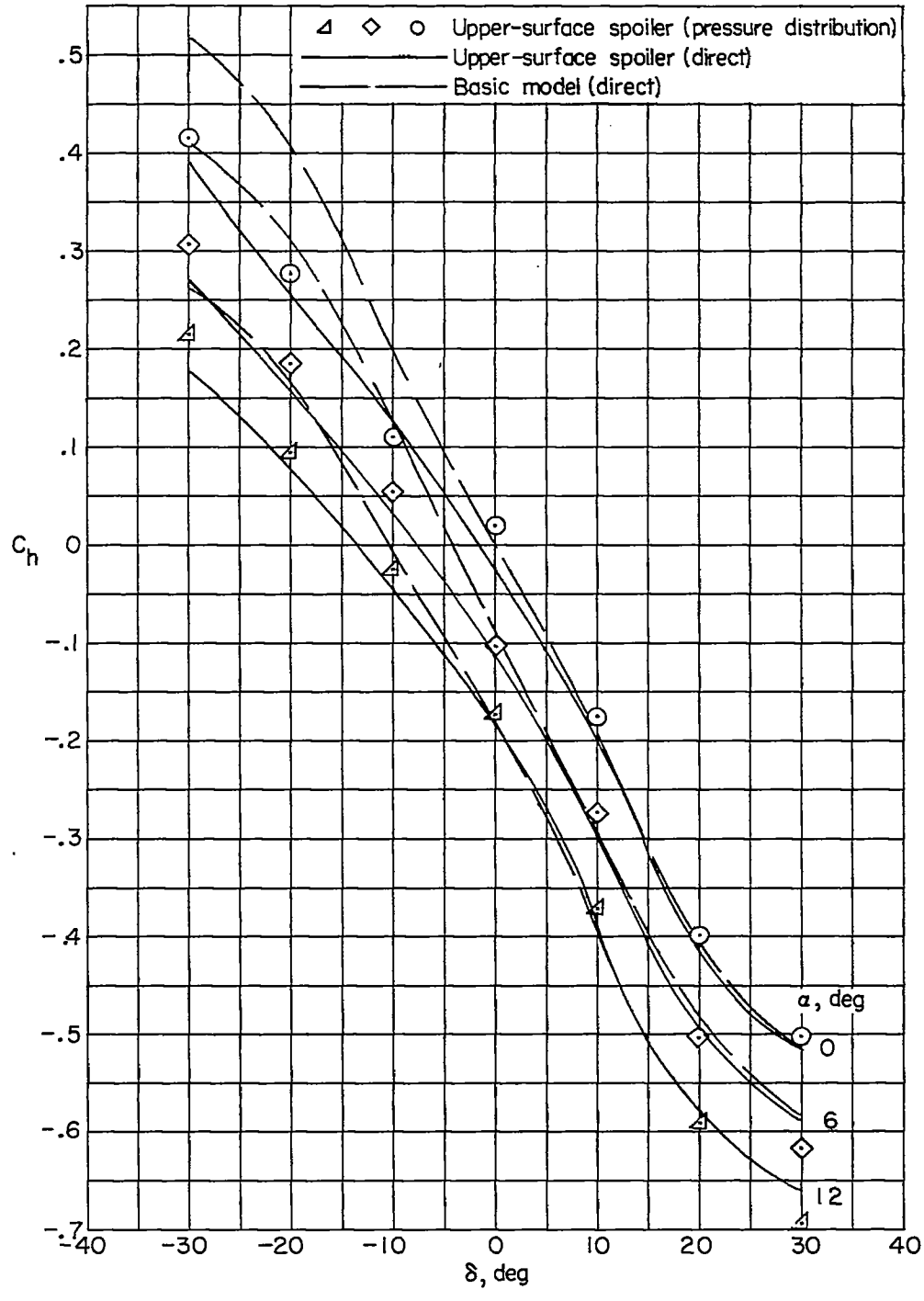

(a) C_h against δ.

Figure 14.- Variation of control hinge-moment coefficient with control deflection and wing angle of attack for the upper-surface spoiler configuration and the basic configuration.

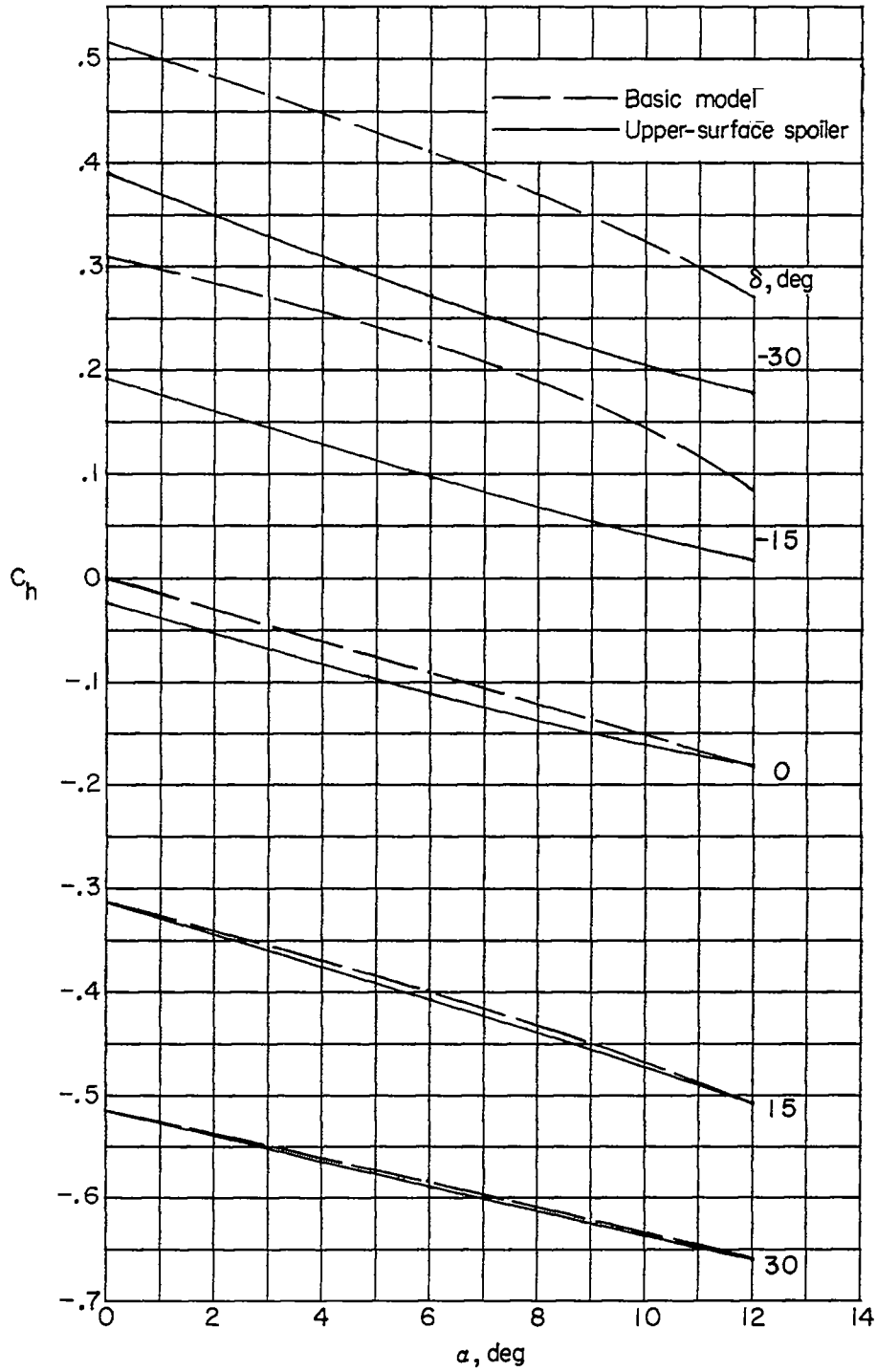

(b) C_h against α.

Figure 14.- Concluded.

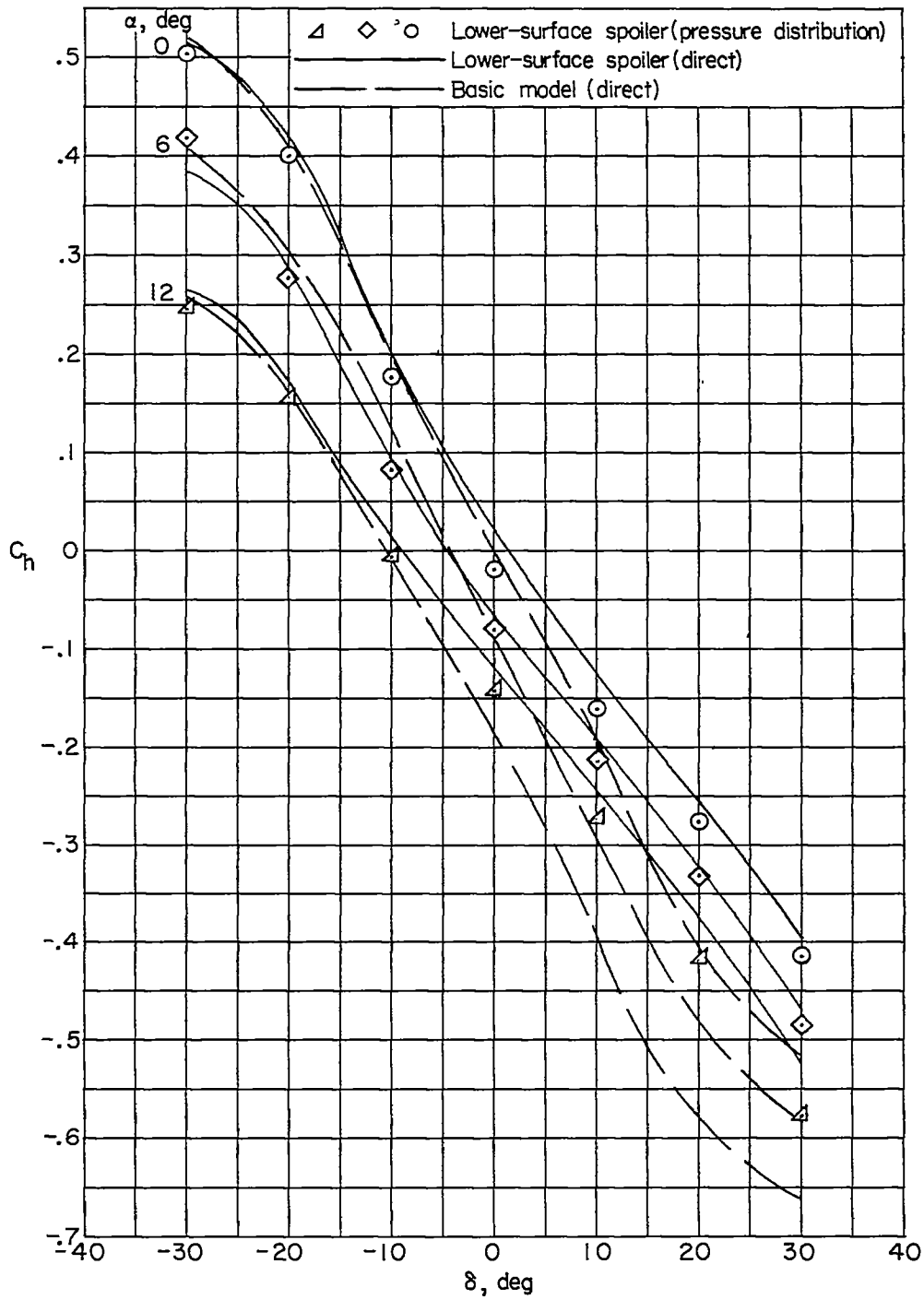

(a) C_h against δ.

Figure 15.- Variation of control hinge-moment coefficient with control deflection and wing angle of attack for the lower-surface spoiler configuration and the basic configuration.

[redacted]

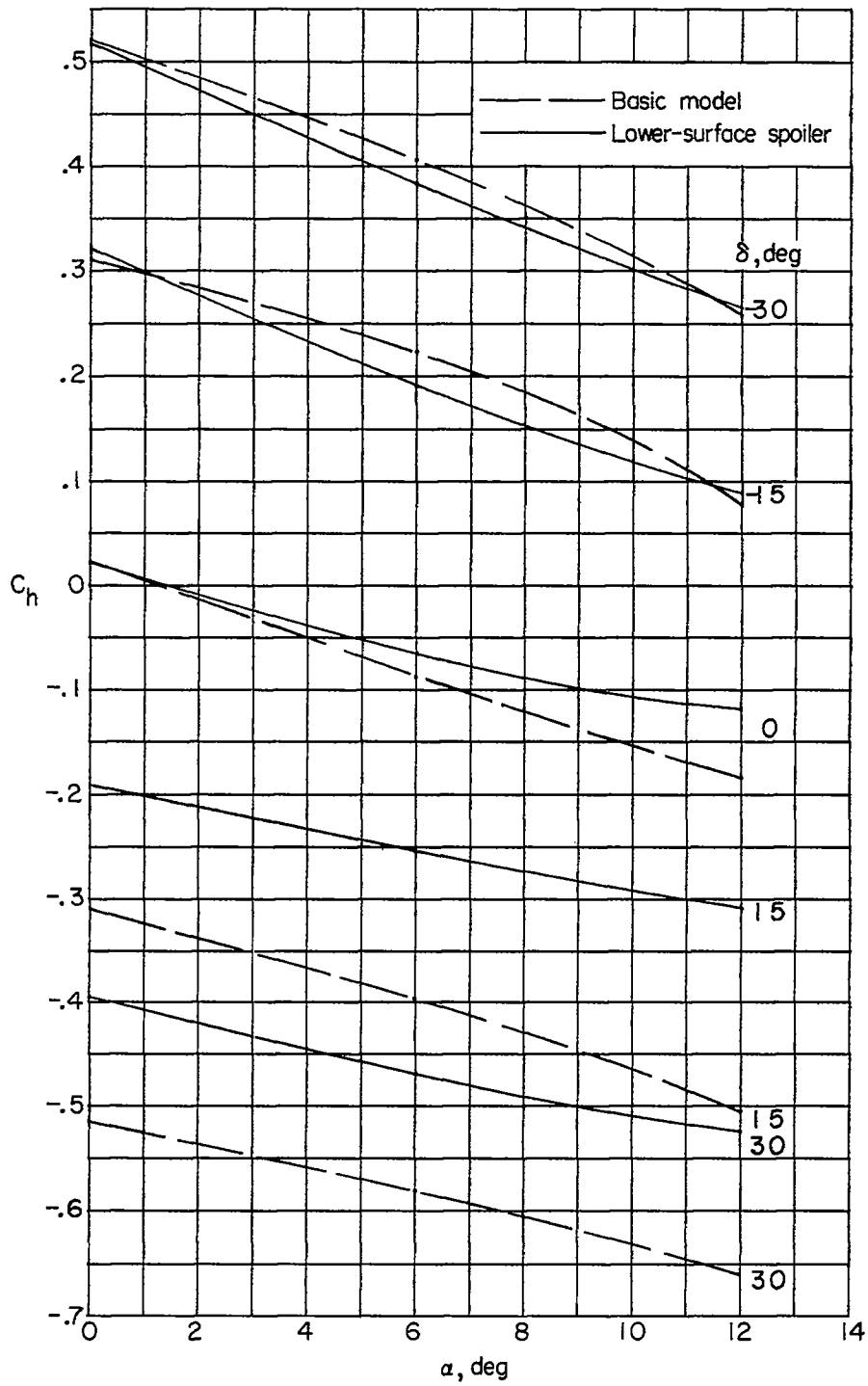

(b) C_h against α.

Figure 15.- Concluded.

[redacted]

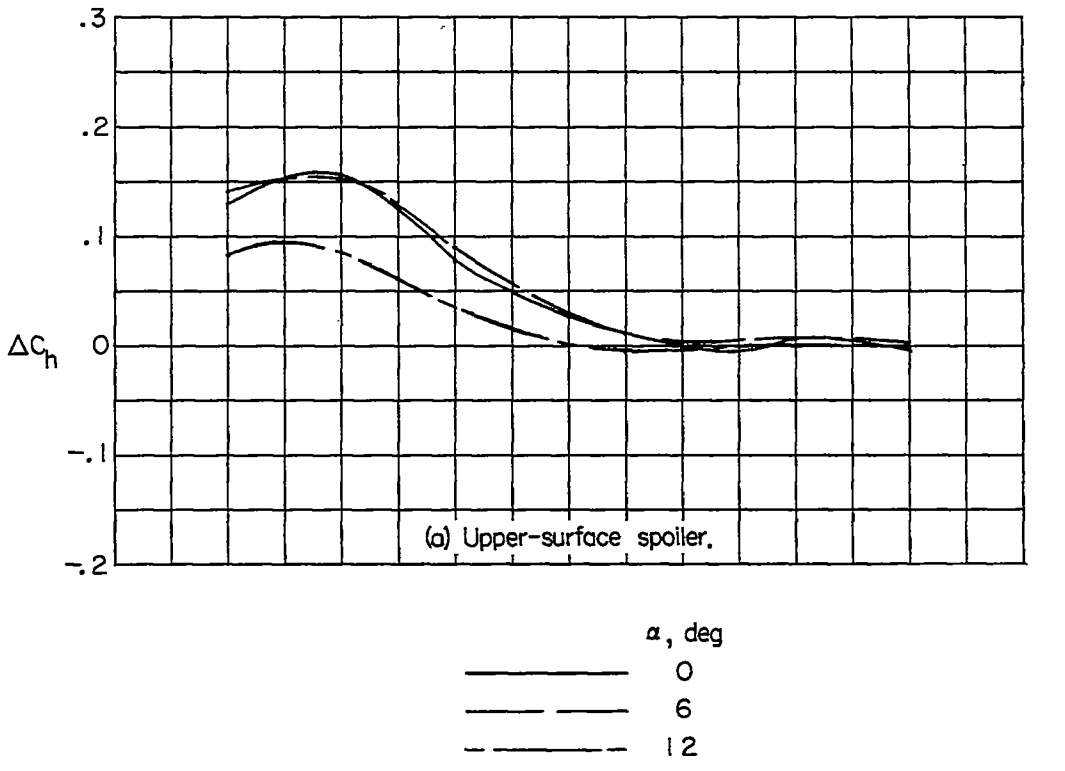

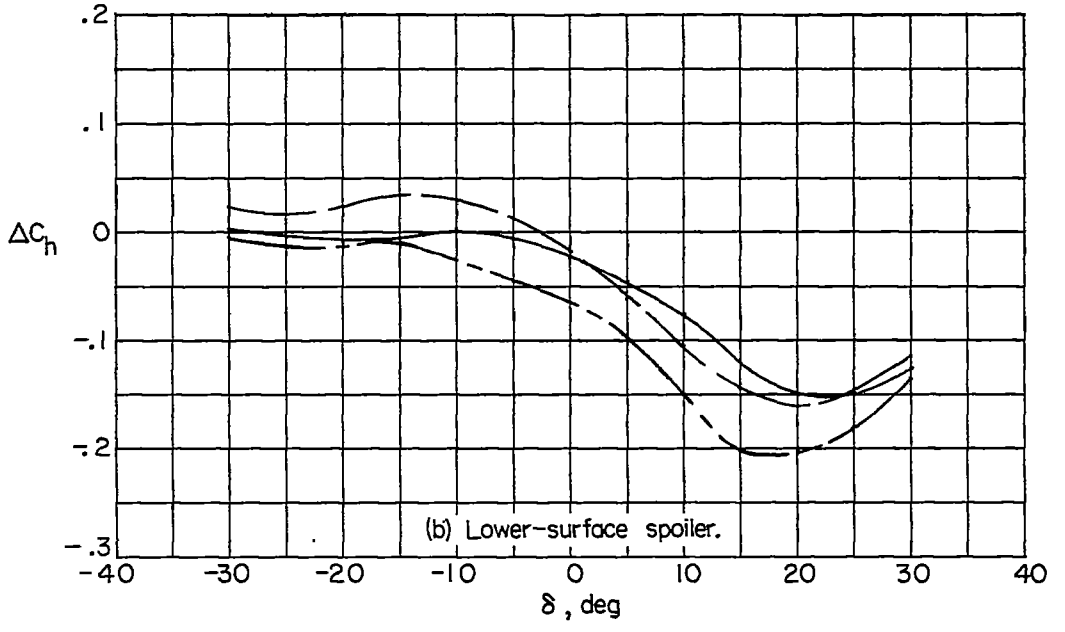

Figure 16.- Variation of incremental control hinge-moment coefficient due to addition of the spoiler on the upper or lower wing surface with control deflection.